Environ Earth Sci (2016)75:684
DOI 10.1007/s12665-016-5456-1

ORIGINAL ARTICLE

Integration of geological investigations with multi-GIS data layers for water resources assessment in arid regions: El Ambagi Basin, Eastern Desert, Egypt

Mohamed Yousif[1] · **Ondra Sracek**[2]

Received: 4 June 2015 / Accepted: 12 February 2016

Abstract Water resources assessment in arid lands is of a particular interest, not only in scientific terms, but also under the concept of sustainable development. The study area (El Ambagi basin), represents a remote arid area with a scarcity of data. The measured effective porosity and permeability revealed high potentialities of the Nubian sandstone and Oligocene sediments. The hydrogeologic setting indicates favorable conditions for groundwater accumulation where there is an opportunity of recharge, and thus, the sustainability of the groundwater. The research approach is based on geological investigations as well as several data layers in the GIS environment including landforms, lithology, slope, soil, morphometric parameters, structural lineaments, and geophysical data. Several specific sites were suggested as targets for future groundwater explorations. The studied basin contains four sub-basins which have an intensive drainage network. The morphometric parameters revealed that they have potential for surface runoff occurrence and also for groundwater recharge. Two of the investigated sub-basins show high hazard degrees and should be protected to avoid flash floods. The estimated runoff volume from a single rainfall event (27 mm) can reach 3316.42×10^3 m^3. Hence, management of rainwater harvesting and protection measures against flash floods are necessary. A future water resources management strategy, based on results of the multidisciplinary study, is proposed.

Keywords Egypt · Eastern Desert · Groundwater · Surface water · Geology · GIS · Remote sensing

✉ Mohamed Yousif
yousif_mohamed80@daad-alumni.de

Ondra Sracek
srondra@yahoo.com

[1] Geology Department, Desert Research Center, P.O.B. 11753, El Matriya, Cairo, Egypt

[2] Department of Geology, Faculty of Science, Palacký University, 17. listopadu 12, 771 46 Olomouc, Czech Republic

Introduction

Water crises in arid regions are rising with the increasing world population and limited water resources (Sultan et al. 2008, 2011). According to the UNEP (United Nations Environment Program 2012), more than two billion people will live under conditions of high water stress by the year 2050, suggesting that water could be a limiting factor for development in several regions of the world. Arid and hyper-arid regions (e.g. the Eastern Desert of Egypt) suffer most from the scarcity of water. The major challenge which is facing Egypt nowadays is the need for better development and management of natural resources, to meet the needs of a growing nation (El-Raey 1998). Therefore, optimal development of the Egyptian deserts and establishment of new communities and settlements are among the most urgent national targets (Yousif and Bubenzer 2015). The present research deals with the following tasks: surface water and flood flash hazard evaluation, elucidation of the factors that affect the occurrence of groundwater, and finally, a future water resources development plan, based on the obtained results from multidisciplinary data layers.

Flash floods can occur in arid regions as a consequence of excessive rainfall and occasionally cause major losses of property and life (Subyani 2009). On the other hand, the demand for groundwater has been increasing over the

Published online: 11 April 2016

years, and the overexploitation and continuous pollution of this vital resource is threatening ecosystems and future generations (Rekha and Thomas 2007). Shallow fracture zone aquifers have renewable water that is recharged by direct infiltration from seasonal precipitation (Sultan et al. 2007, 2011). Groundwater accumulations can be found in crystalline rocks within highly deformed areas such as faults and shear zones (El Baz 1995; El Baz et al. 1998; Sultan et al. 2008; Ruelleu et al. 2010). However, it is difficult to determine the connectivity of fracture systems, or to predict whether groundwater is likely to occur in the fractures (Lewis et al. 2008). Also, sandstone (such as Nubian and Oligocene sandstones) retains a small part of the intergranular pore space that was present before the rock was consolidated; compaction and cementation have greatly reduced the primary pore space. Secondary openings, such as joints and fractures, along with bedding planes, contain and transmit most of the groundwater in sandstone. In most cases, drilling is the only way to confirm the presence of groundwater (Lewis et al. 2008). The identification and location of groundwater resources using remote sensing data is based on an indirect analysis of some directly observable terrain features like geomorphology, geology, slope, land use/land cover, and hydrologic characteristics (Kuria et al. 2012). The scientific approach of this research is based on the combination of multi-geographic information system (GIS) data layers with geological investigations as well as field data to assess available water resources in hyper-arid data-scarce regions. The main objective of this study is to present an approach for assessment of water resources (surface water and groundwater) in an arid, data-scarce remote area, using multi-criteria evaluation techniques on thematic maps for a number of factors with the aid of remote sensing and GIS techniques. Also, the study aims to make recommendations concerning the development of future water resources in the study area. The provided recommendations will have special interest since they will be based on a scientific approach and real data, and can therefore be implemented through the governmental sector or local residents.

Study area

El Ambagi basin is located in the central part of the Eastern Desert of Egypt, approximately 120 km southeast from Hurgada City and drains directly to El Quseir City (Fig. 1). It extends from 33°45′E to 34°15′E and from 25°40′N to 26°15′N, covering about 1500 km^2 and belongs to the arid belt that dominates the Red Sea coastal zone of Egypt. The basin includes four sub-basins: Wadi Bayda, Wadi El Nakhil, Wadi Kareem, and Wadi Abu Hammad. This basin was chosen for the present study for several reasons: (1) El Quseir City receives significant attention from the Egyptian Government to develop this area especially for tourism purposes, but the supplies of water are insufficient to meet the water demands. (2) The study basin is in dire need of water supplies for substantial mining operations, including many sites for phosphate mining activities. This has led to a widespread need for the development and management of regional water resources. (3) The basin receives irregular rainfall events which can damage the main road (El Quseir-Qena), the infrastructure of El Quseir City and the tourist villages. Some of these events have led to floods with loss of life. In 1997, the Quseir City was subjected to a rainy storm caused a destruction of a large number of houses up to 500 homes and cut off roads and means of communication. (4) To date, the investigated basin has not been subjected to detailed hydrogeological studies and many aquifers are not explored yet. (5) The El Ambagi basin represents a case study for a remote arid area with a scarcity of data, which enables us to present a scientific approach for water resources assessment under such conditions. Also, it provides an opportunity to discuss the surface–groundwater relationships in arid regions.

The investigated basin is characterized by a hyper-arid climate (Table 1). It has a very dry summer and a relatively humid cold winter. It has a yearly total precipitation of less than 20 mm, with erratic precipitation and high evaporation. The rainy months are December through February. The mean daily temperatures range between 13.8 and 33.4 °C, while the maximum recorded daily value reaches 45.9 °C. The average annual rainfall is about 3.5 mm and the annual total evapotranspiration (ETo) was 1016 mm for the period of 1985–2014 (Table 1).

Materials and methods

Fieldwork

Fieldwork was performed in January 2015 and aimed to identify the geomorphological and geological settings of the study area. Forty sites in the study area were investigated in detail with regard to geology and one composite section was measured and sampled from surface outcrops. A total of 65 rock samples from different geological units were collected and described. The field data were used for an area-wide interpretation based on Landsat satellite images. A survey of the existing water points was carried out, and six groundwater samples were collected. Here, location (GPS), pH-value, electrical conductivity (EC), and temperature were measured on site. In addition, hydrogeological data such as depth to water table, total well depth, and water-bearing formation depth, as well as

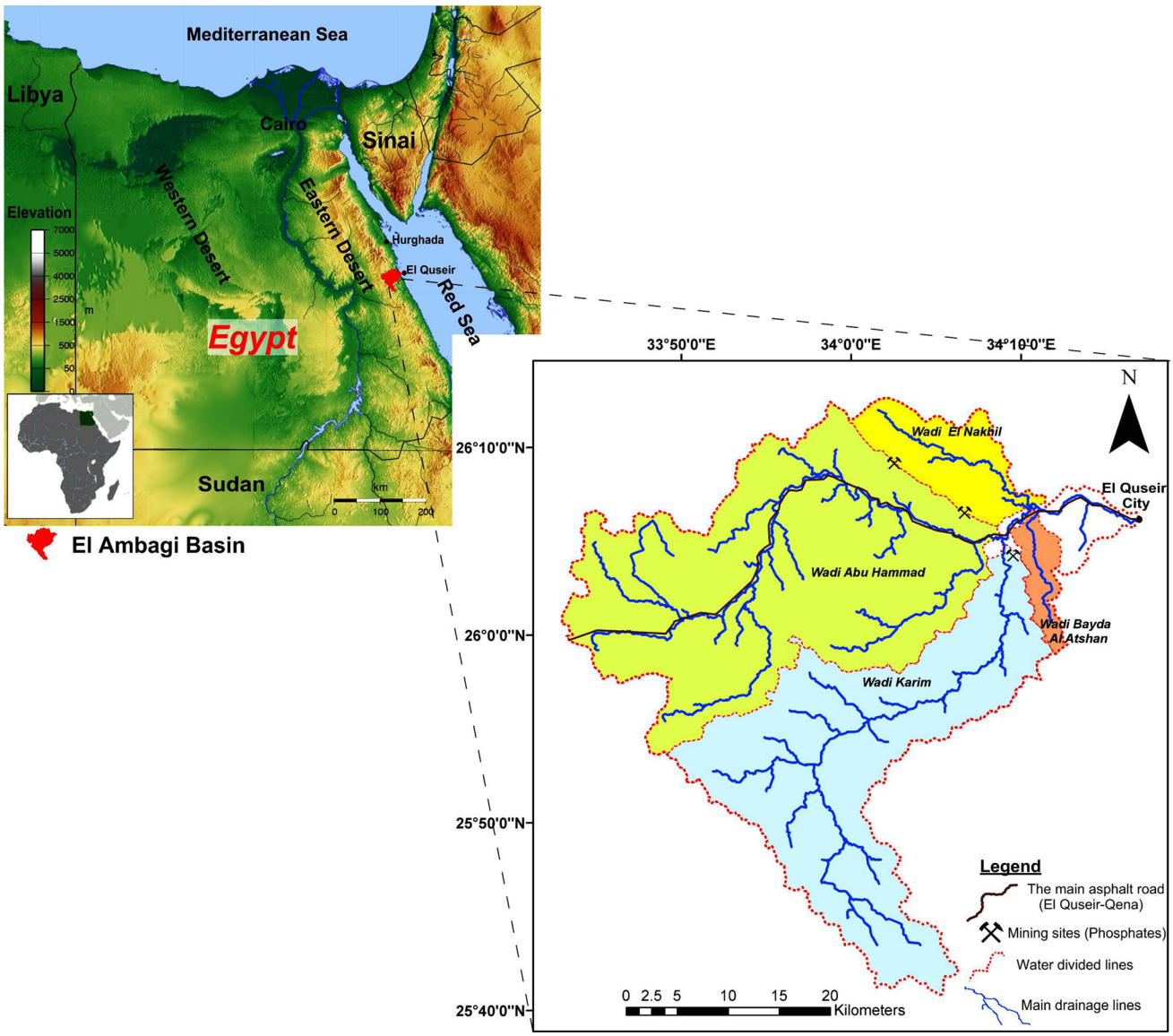

Fig. 1 Map of the study area

corresponding geomorphological units were also determined and measured.

GIS and remote sensing

The Shuttle Radar Topography Mission (SRTM-C) provided the basic data for the current research, as well as satellite images from Landsat 7 (Enhanced Thematic Mapper Plus, ETM+) and Landsat 8 (LC8). The data from satellite images (path 174 and raw 42) was employed for visual interpretation of surface features and geology of the study area as well as the structural lineaments. All the data (SRTM-C, ETM+ and LC8) were projected on the universal transverse mercator (UTM) with the WGS84 datum in GIS for further correlation of features. SRTM-C elevation data are publicly available at a near-global scale at 3 arcsec (~90 m) spatial resolution with 16 m vertical accuracy (Farr and Kobrick 2000). The data were obtained using a dual Space-borne Imaging Radar (SIR-C) C-band wavelength (5.6 cm), which is similar to Radarsat-1 in terms of its penetration ability of the dry sand to portray near-surface features (Ghoneim and El Baz 2007). Although the SRTM-C data have coarser spatial resolution in comparison to ASTER and SRTM-X data, they have proven to be more accurate in revealing the surface topography, especially for drainage evaluation in poorly vegetated areas (Pryde et al. 2007). Hydrophysically, the drainage network represents those points at which runoff is sufficiently concentrated that fluvial processes dominate over slope processes (Mark 1984). The drainage networks

Table 1 Summary of the recorded daily climatic data during the period of (1985–2014)

Parameters	Temperature (°C)		Solar (Mj/m^2)	Relative humidity %	Wind (m/s)	Precipitation P (mm)	Calculated ETo (mm)
	Maximum	Minimum					
Minimum daily value	13.3	1.9	0	10	0.6	0	2.387
Maximum daily value	45.9	30.8	32	54	8.1	26.2	7.18
Mean daily value	33.4	13.8	23.7	40	3.4	0.04	4.554
Standard deviation	7.1	5.6	5.9	0.1	1.1	0.6	0.9
Variances	50.2	31.5	34.7	0	1.2	0.4	0.8
Sum						400	1016
The average annual	25		28	49	2.47	3.5	

Aridity index of the study area and its vicinities

Station	Temperature (°C)		Average annual P (mm)	Aridity index Q	State
	T_{max}	T_{mim}			
El Quseir	33.4	13.8	3.5	3.7	Hyper-arid
Hurghada	33.3	9.7	3.6	3.5	Hyper-arid

The extreme single rainfall events during the period of (1985–2014)

Date	Temperature (°C)		Precipitation P (mm)	ETo (mm)	Rainfall surplus P–ETo (mm)
	Maximum	Minimum			
22-03-91	19.93	15.10	27.00	5.67	21.33
01-11-92	22.30	16.32	20.94	4.27	16.66
19-05-93	25.79	18.92	14.78	6.48	8.29
21-12-93	20.31	16.99	15.28	3.95	11.33
01-01-94	26.76	16.82	7.00	3.93	3.07
02-01-94	20.87	16.34	13.12	5.67	7.45
02-11-94	24.69	20.86	23.07	4.38	18.70
19-03-95	22.62	15.02	7.00	5.32	1.68
26-05-95	33.75	21.73	18.89	9.19	9.70
14-01-97	21.78	17.66	10.00	3.65	6.35
18-01-10	20.07	13.40	14.18	5.73	8.45
29-12-10	25.92	16.30	17.99	5.98	12.01

Sources: Global Weather Data for SWAT (daily records), Meteorological data of Hurghada and El Quseir, the Egyptian Meteorological Authority, *ETo* evapotranspiration (calculated through Penman–Monteith equation)

can be derived from a variety of sources including topographic maps, aerial photographs, field survey, satellite images and recently from digital elevation models (DEM). The manual extraction of drainage networks is a very inconsistent process even within the same network (El Bastawesy 2007; El Bastawesy et al. 2009). The processing of SRTM-C started by constructing a mosaic to extract the watersheds of the study area. The hydrology tools of ESRI Arc GIS v.10 were employed to identify and fill all sinks in the resulting mosaic. The flow direction grid was extracted based on the D8 flow direction algorithm (Foody et al. 2004), next, the drainage network was extracted by calculating the flow accumulation for each cell. The density of the drainage network was defined using an appropriate threshold of 300 cells of contributing drainage area. The following layers were obtained from the digital elevation model (DEM) analyses: slope, flow direction, drainage lines, basins, and shaded relief. Moreover, the DEM data were used to create a three-dimensional layer (3D) to illustrate the main landforms as well as geological and geomorphological units. The Landsat 8 image (LC8, 2014), which has a panchromatic spatial resolution of 15 m, contains 11 bands, was used in combination with the Harmonized World Soil Database v 1.2 (2009) to identify the main soil units of the study area (band combination 432, 764 and 543).

Landsat GeoCover ETM+ 2000 (ETM-EarthSat) provided by Global Land Cover Facility (http://glcf.umiacs.

umd.edu/data/mosaic/) with a spatial resolution 15 m, was used for field investigations and the geological map (1:500,000, Conoco, 1987) to identify the geology of the study area (band combination 742). The GeoCover ETM+ is a global set of regional images to create a mosaic from the Landsat GeoCover data set which was designed at the NASA Space Center. Geological features like faults can be seen in the bands 754 and 741 of the ETM+. Enhancement techniques like filtering were applied, e.g. edge detection through convolution filtering in ERDAS IMAGIN 9.3, which depends on variations of digital pixel values of the image (Gupta 2003). The geological map (Conoco 1987) and the works of El Shazly et al. (1981) were used with the ETM+ and DEM to extract the structural lineaments which were overlaid onto the shaded relief map. The interpretation of the Landsat images was done using ERDAS IMAGINE (ver. 9.3) where the images were first re-projected to the study area, and then imported into the ESRI ArcMap GIS 10. The spatial analysis of various data was carried out using the ArcGIS 10 software, to interpolate the data spatially and to convert the data to the requested layers. All maps in the present research were prepared in the ArcGIS 10 environment.

Measuring of porosity, permeability, and microfacies analyses

The effective porosity and permeability were determined for 20 sandstone samples from Nubian and Oligocene formations. These analyses were performed in the Core Analysis Lab of the Egyptian Petroleum Research Institute. A helium porosimeter (Heise Gauge type) was used for porosity determination. Thin sections of 15 rock samples of different geologic ages were prepared and carefully examined microscopically to identify their petrographic constituents and microfacies associations. Thin sections of the sandstone samples were stained by blue dye to investigate the porosity and permeability. Also, the environmental deposition, the paleoecological conditions, the origin of the rock constituents, and the digenetic alteration processes were investigated. The microfacies associations were compared with the standard microfacies types of Wilson (1975), and the facies zones of Flügel (1982), for the recognition of the paleo-environment of the studied rocks. Knowledge of the depositional environment (e.g. marine, fluvial or terrestrial) of the aquifer rock is important in terms of rock-groundwater interactions.

Rainfall analyses

Since the runoff volume is associated with the average of precipitation, the detailed data during long and short periods should be analyzed. Therefore different datasets were obtained from the following sources:

1. Daily records during the period of 1985–2014; these records include the following parameters: Temperature (maximum and minimum), solar insolation, relative humidity, wind speed, and precipitation. These data were obtained from the Global Weather Data database for SWAT (http://globalweather.tamu.edu/).
2. The annual precipitation during the period of 1945–2010 (NCEP 2015).
3. Monthly accumulated rainfall during the period of 1985-2015. The data were obtained from the Tropical Rainfall Measuring Mission (TRMM) with a spatial resolution of 0.25 × 0.25 for (3B43), which can be accessed with the GES DISC Mirador system (http://mirador.gsfc.nasa.gov). Analyses and visualizations used in this study were produced with the Giovanni online data system, developed and maintained by the NASA GES DISC centre.
4. Meteorological data of Hurghada and El Quseir, i.e. unpublished data from the Egyptian Meteorological Authority during the period 1980–2010.

The daily records were used as input data and imported to the Instat+ statistical software (ver. 3.036). This statistical software was used to facilitate the analysis of the many records, where each of the following output parameters were included: Minimum daily value, Maximum daily value, Mean daily value, Standard deviation, Variances, summation, and average annual values. Also, it provided the calculation of evapotranspiration through the Penman–Monteith equation (FAO-56 Penman–Monteith equation, Allen et al. 1998). The other datasets were used to determine the main rainfall events which affected the study area.

The annual rainfall occurs sporadically and for short periods as storms. Floods can occur at intervals, so surface runoff is important, but in some years no rainfall occurs. The aridity index of the study area is determined using Emberger's equation (1955) as follows:

$$Q = P/[(T_{\max} + T_{\min})(T_{\max} - T_{\min})]1000 \quad (1)$$

where Q is the aridity index, P is the average annual precipitation (mm), $T_{\max}$ is the mean maximum temperature of the hottest months (°C), and $T_{\min}$ is the mean minimum temperature of the coldest month (°C). Accordingly, the study area is considerably hyper-arid since the aridity index is much lower than 20.

Morphometric analyses

Morphometric analysis provides a quantitative description of the watershed geometry to understand the initial slope or differences in the rock hardness, structural controls, recent

diastrophism, geological and geomorphic history of watersheds (Strahler 1964; Clarke 1966). This can be achieved through measurement of linear, aerial, and relief aspects of the watershed and its slope contributions (Nag and Chakraborty 2003). A quantitative morphometric analysis was carried out in the studied basins and catchment areas by the use of GIS to determine their linear, areal, and relief aspects.

A total of 22 morphometric parameters were determined (Table 4). The interpretation of the obtained values for the different parameters was carried out according to the schemes of Horton (1932), Schumm (1956), and Strahler (1953, 1964) for an evaluation of the surface hydrology with regard to the flood hazard in the studied basins. Ten parameters were identified to have a direct effect on flash flood events: watershed area (A), drainage density (D), stream frequency (F), basin shape index (Ish), relief ratio (Rr), ruggedness ratio (Rn), slope index (Sin %), weighted mean bifurcation ratio (WMRb), length of overland flow (Lo) and sinuosity (Si). All these parameters have a directly proportional relationship with the hazard morphometric parameters except for (WMRb), (Lo) and (Si) which show an inverse correlation. A hazard scale number starting with 1 (the lowest) to 5 (the highest) has been assigned to all parameters. The distribution of the hazard degrees for the studied drainage basins have been carried out as follows (comp. Bajabaa et al. 2013):

- Determination of the minimum and maximum values of each morphometric parameter for all drainage basins and their sub-basins.
- Assessment of the actual hazard degree for the all parameters which are located between the minimum and maximum values depends on a trial to derive the empirical relation between the relative hazard degree of a basin with respect to flash floods and the morphometric parameters.
- Equal spacing or simple linear interpolation between data point procedure was chosen.

Assuming a straight linear relation exists between the sampling points, the intermediate values can be calculated from the geometric relationship (Davis 1975; Sewidan 2000):

$$\text{Hazard degree} = \frac{4(X - X_{\min})}{(X_{\max} - X_{\min})} + 1 \quad (2)$$

For the parameters which show an inverse correlation, the hazard degree was calculated using the following equation:

$$\text{Hazard degree} = \frac{4(X - X_{\max})}{(X_{\min} - X_{\max})} + 1 \quad (3)$$

where X is the value of the morphometric parameters to be assessed for the hazard degree for each basin, and $X_{\min}$ and $X_{\max}$ are the minimum and maximum values of the morphometric parameters of all basins, respectively. The summation of the hazard degrees (Eqs. 2, 3) for each basin represents the final flood hazard for that basin.

Estimation of surface runoff

The curve number (CN) is a hydrologic parameter used to describe the surface water runoff potential for a drainage area, which is a function of land use, soil type, and soil moisture. The present study used the curve number which was tabulated in USDA-SCS (1986) acceding to the soil and land use of the studied sub-basins.The runoff volume estimation is expressed mathematically as follows (USDA-SCS 1972, 1986):

$$Q(\text{actual runoff}) = (P - \mathrm{I}_a)^2 \Big/ (P + 0.8S) \quad \text{for } P > 0.2S \quad (4)$$

$$I_{\mathrm{a}} = 0.2S \quad (5)$$

A dimensionless curve number CN is defined such as $0 < \mathrm{CN} > 100$

$$S = (25400/\mathrm{CN}) - 254 \quad (6)$$

where P is the total rainfall, I_{a} is initial abstraction, and S is potential maximum retention. On the other hand, the weighted mean curve number (CN) is calculated for the areas which have mixed curve number values as follows:

$$\text{Weighted CN} = (\mathrm{CN_i} \times A_{\mathrm{i}})/A \quad (7)$$

where $\mathrm{CN_i}$ is the value of curve number for a partial area A_{i}, and A is the total basin area. The total runoff volume for an area

$$\mathrm{Qv\,m^3} = Q(\text{actual runoff}) \times A\left(\text{area m}^2\right) \quad (8)$$

From Eqs. 4, 5 and 6, the actual runoff in the present study was estimated for each basin and the total volume of the runoff was estimated using Eq. (8).

Geophysical data

The available geophysical data did not cover the entire studied basin. These data were obtained from different sources including the land magnetic and geoelectrical surveys. Initially, the total magnetic intensity of the earth's magnetic field (TMI) was measured and recorded, the Vertical Electrical Sounding (VES) method and resistivity tomography were also applied. The sources of the data are as follows: an unpublished report prepared by the Desert Research Center (MPGAP 1990) and Khaled (2002, 2007). In addition, the unpublished report (Red Sea governorate and Desert Research Center, Frame of Development of

Bedouins Communities 2007) provided data about the Wadi El Nakhil sub-basins. The data were combined and the basement relief was obtained from the land magnetic survey (four profiles) with the geoelectrical data (32 VES).

Water chemistry analyses

In total, 6 groundwater samples were analyzed for major ions at the laboratory of the Desert Research Center (DRC, Cairo, Egypt) by ion chromatography (ICS-1100, Dionex, Sunnyvale, CA, USA). The analyzed major ions included sodium (Na^+), potassium (K^+), calcium (Ca^{2+}), magnesium (Mg^{2+}), carbonate (CO_3^{2-}), bicarbonate (HCO_3^-), chloride (Cl^-) and sulfate (SO_4^{2-}).

Results

Geomorphologic aspects

The study area is subdivided into two major morphological units: highlands and lowlands. The highlands include the Red Sea terrains and the tableland, while the lowlands include the coastal plain and drainage basins (Fig. 2).

Red sea terrains

The Red Sea Terrains range in elevation between 500 m to more than 1000 m above mean sea level. The Red Sea Mountains are composed primarily of Pre-Cambrian rocks that are crystalline in character (igneous and metamorphic rocks) and extending more or less parallel to the Red Sea at a comparatively short distance inland from the coastline. However, they do not form a continuous range, rather a series of mountain blocks, which are more or less adjacent and dispose a linear trend parallel to the coastline with some detached masses and peaks. The Red Sea Mountain Ranges themselves are not folded; instead, they have been formed due to a large extent by uplifting the margins of the rift. Regarding the erosion cycle, Hamdan (1980) assumed that the physiographic characteristics of the Red Sea Mountains manifest a youth stage character. This is based on the fact that incised wadis separating broad large blocks and wadi gradients are irregular with waterfalls, rapids, and lakes, which are all formed in response to lithological variations and structural lineaments.

Tablelands

Tablelands are located either on the western border of the coastal plain or inland occupying the intermountain basins. They consist of Cretaceous-tertiary rocks, which are formed mainly of limestone, sandstone, chalk, and conglomerates constituting low parallel escarpments. The coastal tablelands border the basement rocks from the east and attain an elevation of about 450 m.a.s.l. The rocks are slightly tilted seawards with general slopes varying between 5° and 20° and constituting cuestas, tabular mesas, and inselbergs. The inland tablelands are preserved within morphotectonic or geosynclinal depressions. They are remnants of earlier rock covers, which had existed before the area was exposed to orogenic processes. They are situated east of longitude 34°E, while to the west of that longitude most of the sedimentary rock cover has been completely eroded and removed. They have the same trend NNW-SSE as well as the same rock formation but, in contrast to the coastal hills, they are significantly structurally controlled. As a consequence, they comprise distinct long sharp scarps that are a function of dip, thickness, and relative resistances of the rock strata. The form of Gebel Duwi is considered a cuesta owing to moderate dip with a notable difference in steepness as well as length of the front and back slopes. As a whole, the tablelands have experienced intensive faulting and folding that gave rise to distinctive landforms along the coastal plain and within the intermountain depressions.

Coastal plain

The coastal plain represents the eastern narrow strip of the study area, parallel to the Red Sea coast. It extends in a NW–SE trend and is formed by coalescing alluvial fans and coral reefs. The width of the coastal plain varies from 1 to 5 km, depending on the distance between the Red Sea Mountains and the coastline. The height of the coastal plain varies greatly between 0 near the coastline to 100 m above sea level (a.s.l) at the foot-slopes of the Red Sea Mountains.

Drainage Basins

The El Ambagi basin includes 4 sub-basins: Wadi Bayda, Wadi El Nakhil, Wadi Kareem, and Wadi Abu Hammad. Most of them cut through the morphotectonic or the geosynclinal depressions, which are oval in shape and filled with alluvial sediments and blown sands. Generally, drainage networks are convergent due to geologic structure and rugged relief. Therefore, consequent and obsequent wadis with dendritic and trellis patterns are common. Hamdan (1980) assumed that the Red Sea drainage system had been formed during Pleistocene and Pliocene times, if not in Miocene, as the time when the Eonile was developed (Said 1993). Therefore, drainage networks of the study area could be considered as one of the oldest and most complex drainage systems in Egypt. Today, few wadis of the Eastern Desert ever convey streams of running water.

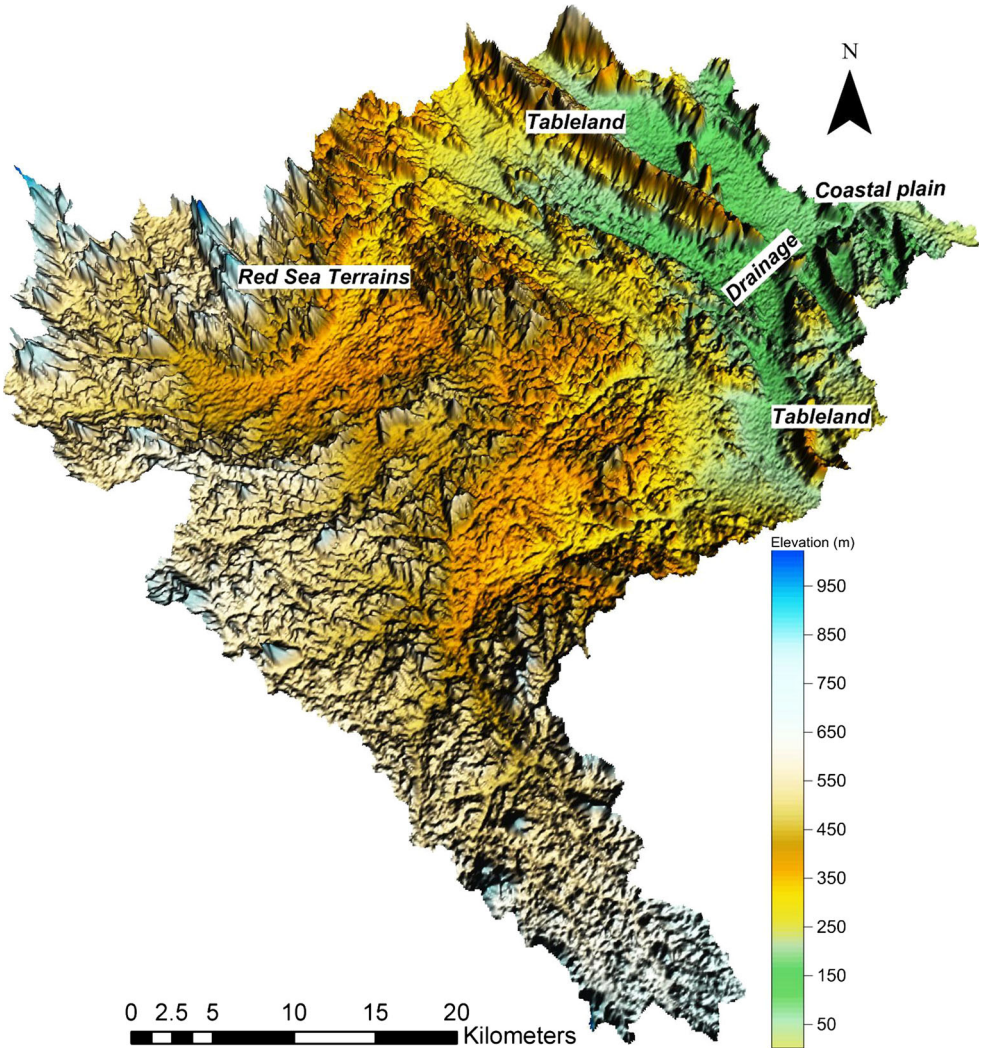

Fig. 2 Three-dimensional (3D) map showing the main landforms of the study area

Generally, it happens only for short periods after exceptionally heavy rainfall in the mountains, which occurs at intervals of several years. However, many wadis contain a certain amount of natural vegetation, which allows grazing of different animals of the Bedouins people.

Geological investigations

Lithostratigraphy

Stratigraphically, the catchment area of El Ambagi basin is dominated by a wide variety of rocks, i.e. the Precambrian basement rocks which are covered by Cretaceous, Tertiary and Quaternary sediments. According to the geologic map of the study area (Conoco 1987, Fig. 3), the measured composite section of Gebel Duwi (Fig. 4), and the works of Youssef (1957) and Said (1992), the general stratigraphy of the study area can be summarized from older to younger as follows:

Pre-Cambrian rocks (basement)

The Pre-Cambrian rocks form a complex of igneous and metamorphic rocks. They are mainly composed of gneisses, schists, serpentinite, gabbros, and granite. These rocks are characterized by many sets of fractures and a number of acidic to basic dykes cut the older basement rocks.

Sedimentary rocks (Upper cretaceous-oligocene)

These sediments form isolated outcrops as in Gebel Duwi. The succession of these outcrops from bottom to top is as follows:

– *Taref formation, Nubian sandstone (Turonian–Santonian):* The Nubian sandstone represents the oldest sedimentary beds resting uncomfortably over the basement complex rocks and forming low topographic hills. It is built of non-fossiliferous sandstone with

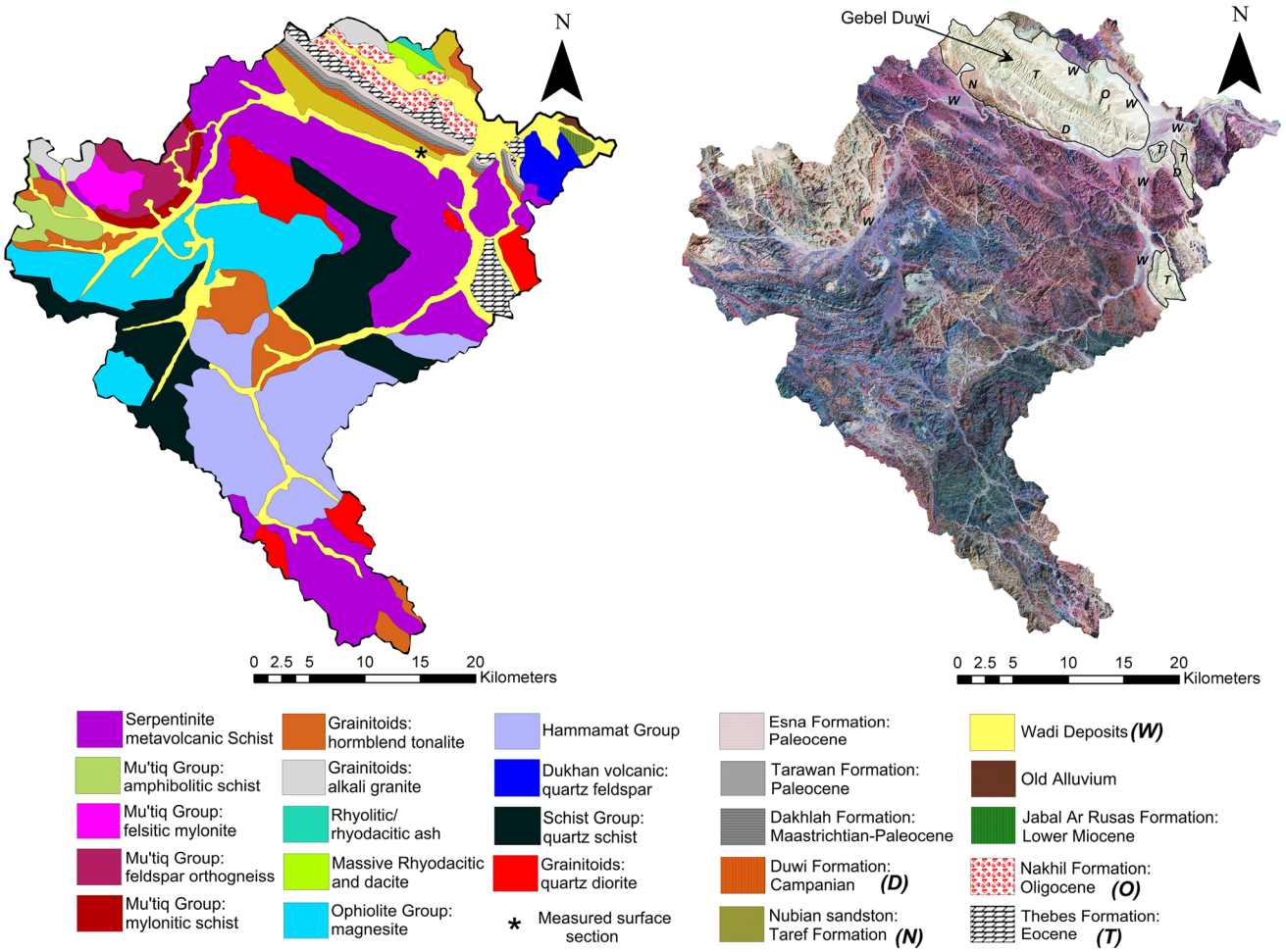

Fig. 3 Geologic setting of the study area, extracted from geology maps (Conoco 1987) and Landsat images (Landsat GeoCover ETM+)

intercalations of mudstones. The measured thickness in the study area reaches 85 m.

- *Duwi (phosphate) formation* (Campanian): is made of limestone with three phosphate horizons separated by beds of marl, shale, and oyster limestone. The phosphate-rich rock is dark in color and has silicified phosphatic nodules. It has a thickness varying between 6 and 10 m.
- *Dakhla formation* (Masstrichtian–Paleocene): This formation is composed of marl and shale. In Gebel Duwi, its measured thickness reaches up to 100 m and can be subdivided into a lower marl member (Hamama) and an upper shale member (El Beda).
- *Tarawan formation* (Paleocene): The formation is made up of marl and marly limestone, ranging in thickness from 6 to 10 m.
- *Esna formation*: This formation is made up of grey laminated shale with a middle limestone member of about 50 m thick in Gebel Duwi.
- *Thebes formation* (Eocene): This formation uncomfortably overlays the Esna Shale. It is made up of limestone with flint bands or nodules and interbedded chert concretions, which forms the important topographical features of Gebel Duwi (about 285 m thick). The Thebes Formation forms old white cliffs running sharply to ground level with a dip slope of 10° to 15°.

Microfacies analyses, porosity and permeability

Petrographically, the sandstones of the Taref Formation (Nubian sandstone) and Nakhil Formation are composed mainly of quartz arenites and less commonly quartz wackes. Quartz grains represent the main constituent of both formations. The quartz arenites of both formations are mostly clear, medium to coarse grained, moderately sorted, sub-angular to sub-rounded and occasionally rounded. Quartz grains are sub-equant, rarely elongated, randomly oriented and have variable degrees of packing (mainly open packed). The main difference between the sandstones of both formations is the ferruginous cementation which was recorded only in the Nubian sandstone. The facies distribution and microfacies examination show that these

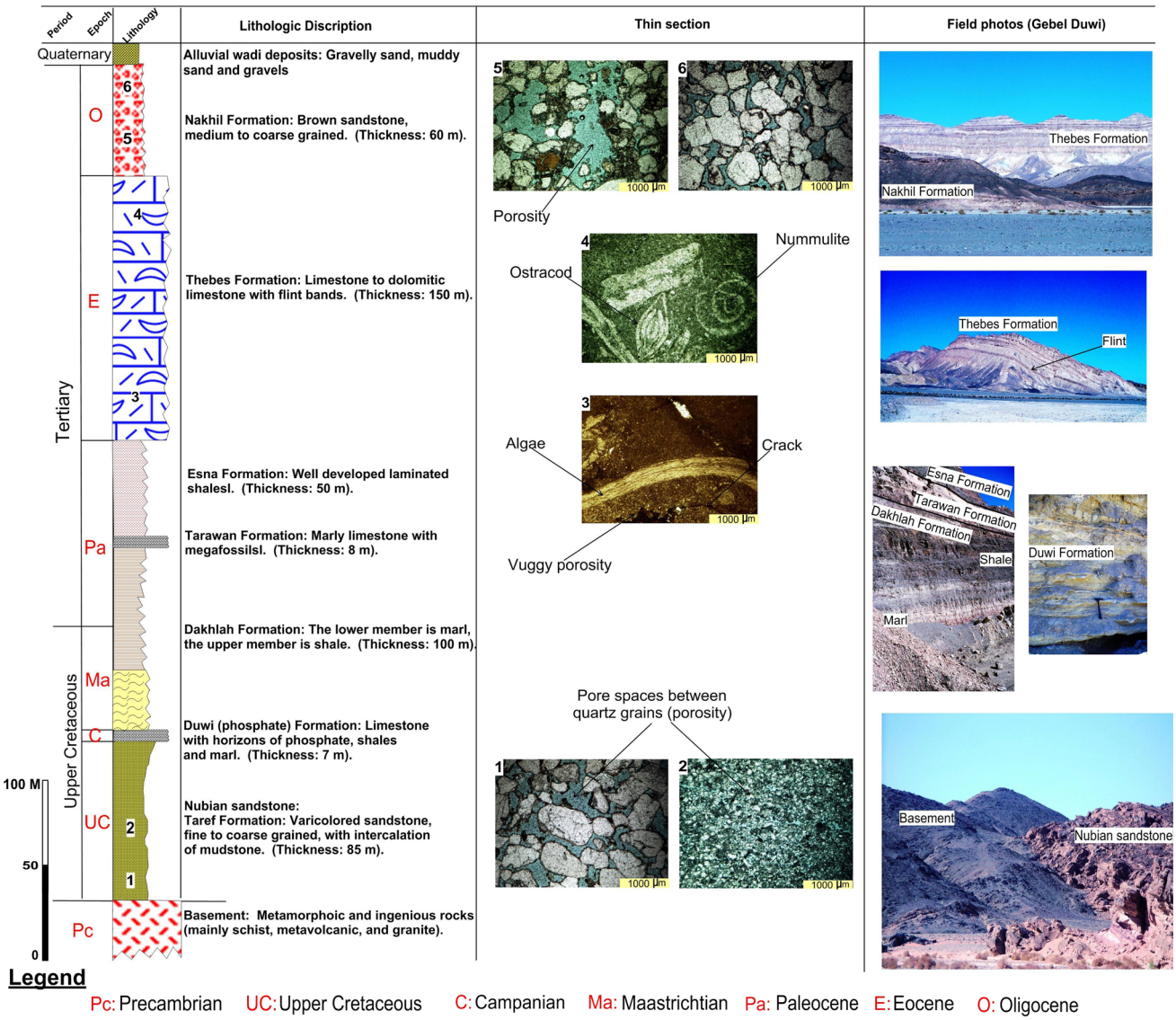

Fig. 4 Composite stratigraphic section of Gebel Duwi, supported by thin section photos and field photographs

sandstones are fluvial-marine sediments. The weathering products of the source rocks were transported to the basin of deposition mainly by rivers, during a low stand of sea level. This is indicated by the sedimentary structures (cross lamination and fining upward sequence). These sandstones were deposited most probably in a river environment with intermittent beach contribution. The investigated sandstone seemed to be affected by various types of diagenesis such as pressure solution, cementation and compaction. Primary porosity is rarely noted in a few samples while secondary porosity is developed in sandstones during diagenesis by pressure solution and leaching processes leaving intergranular porosity and also through tectonic movements producing fractures in the rocks. The investigation of porosity and permeability of stained sandstones (blue dye) from both formations reveals the possibility of these rocks to be water-bearing formations. The dark brown coloration of the matrix is caused by iron stains that partly fill the cracks and reduce the porosity. The presence of abundant foraminifera of benthonic and planktonic species in the studied formation implies deposition in variable depth. Moldic and vuggy porosity were noted between individual crystals while fracture porosity formed through tectonic movements, collapse, and slumping of beds as a result of dissolution. The fractures are different in length and width; it is noted in some thin sections that they are filled by crystals which has led to reduced permeability.

The measured effective porosity of the Nubian sandstone ranges between 7.3 % in the middle part and 24 % in the lower and upper parts (average 20 %). However, it

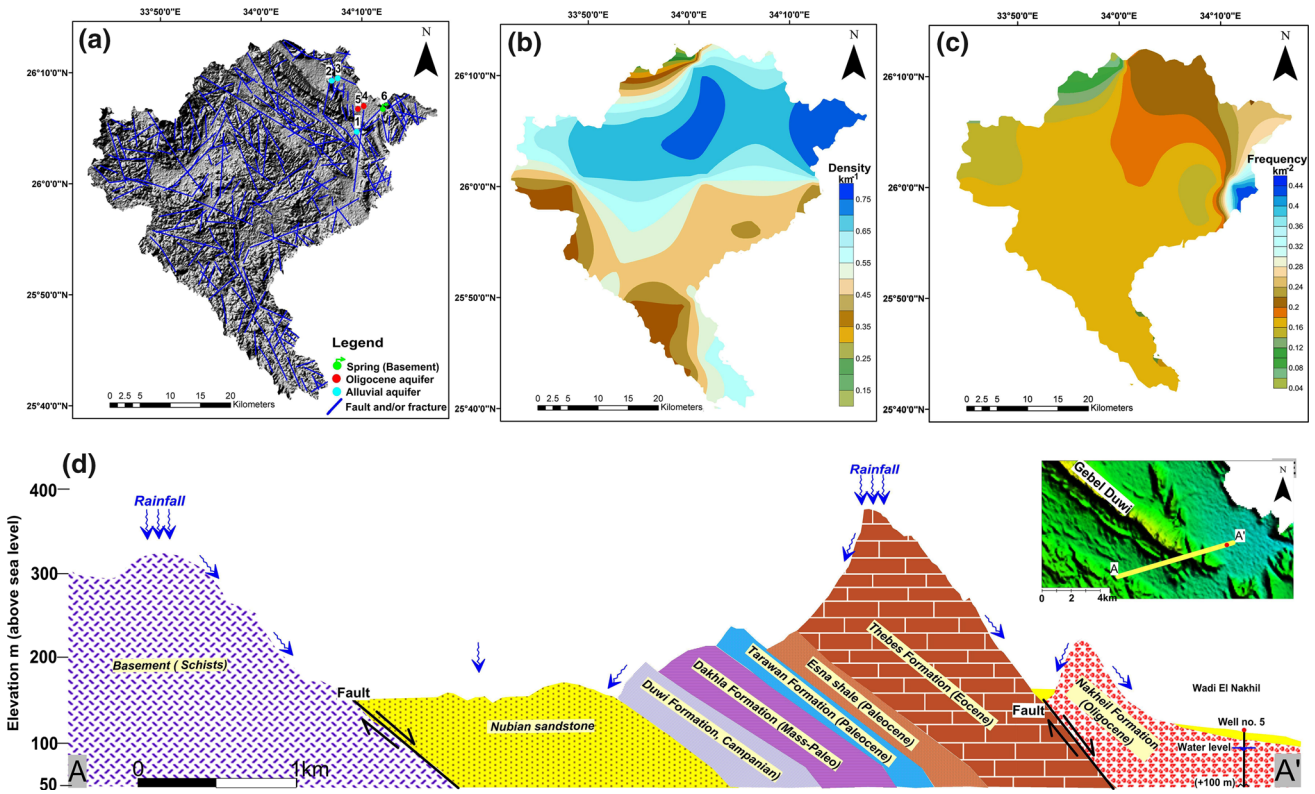

Fig. 5 Structural setting of the study area. **a** The structural lineaments and groundwater wells plotted together over a hilly shaded map. **b** and **c** Two contour maps of the lineament density and frequency showing the regions most affected by structure lineaments. **d** Cross-section (A–A') showing the surface outcrops and the potential recharge and runoff zones

ranges between 22.3 % in the lower part and 11 % in the upper part of the oligocene sandstone (average 19.8 %). The permeability values vary between 1×10^{-16} and 6×10^{-16} m^2 in the Nubian sandstone, while the values range between 3.5×10^{-12} and 6.6×10^{-16} m^2 in the oligocene sandstone.

Delineation of structural lineaments

The delineation of structural lineaments of the studied basin shows that the area was affected by several sets of faults. The main trend of lineaments is NW–SE followed by NE–SW and E–W directions (Fig. 5). The lineament density of the study area varies between 0.15 and 0.74 km/km^2, while the lineament frequency ranges between 0.15 and 0.42 km^{-2}. The structural lineaments are concentrated in the vicinities of the Wadi El Nakhil and Wadi Byada sub-basins and to the west of Gebel Duwi. The exposures of the basement rocks and Eocene rocks (Thebes formation) are highly fractured by cracks and joints that are mostly connected. Also, the other exposures of Nubian sandstone and Oligocene sediments (Nakhil formation) are fractured to a lesser degree than the others. It is assumed here that the drainage is structurally controlled and well developed within the areas where lineaments are abundant. The cross-section (A–A') shows that the exposures of the Gebel Duwi are bound by two faults of NW–SE directions (Fig. 5).

Hydrogeological setting and subsurface data

Investigations of the spatial distribution of the existing wells are important in the developing of groundwater resources. Field survey of the productive wells indicated that they exist mainly at the downstream portions of the sub-basins (Fig. 5). These sub-basins are located in extensional fracture zones. The groundwater exploration of the study area is still very limited and only 5 active wells, in addition to one natural spring, were recorded (Table 2). The water-bearing formations are distinguished as Quaternary alluvial, Oligocene sandstone and Pre-Cambrian basement rocks.

Quaternary alluvial aquifer

The Quaternary deposits are composed of detrital alluvial sands, pebbles, boulders and rock fragments with thicknesses varying from centimeters to 20 m. These deposits

Table 2 Hydrogeological and chemical data of the groundwater wells in the study area

Well no.	Well name	Location		Aquifer	Total Depth (m)	Depth to water (m) from ground	Type of well	Hydraulic parameters[a]				
		Long. "N"	Lat. "E"					D (m^3/h)	PD (h)	T (m^2/day)	SD (m)	HC (m/day)
1	Bir Al Bidah	34.15	26.07	Alluvial	7.5	5.2	Hand dug					
2	Nakhil 1	34.11	26.15		5	3.75	Hand dug					
3	Nakhil 2	34.12	26.15		3	1.5	Hand dug					
4	Nakhil 3	34.16	26.10	Oligocene	166	17.5	Drilled	65.5	3	1098.8	139.9	7.79
5	Nakhil 4	34.15	26.11		157	17	Drilled	69	5	863.2	148.2	5.82
6	Ain Al-Ghazal	34.19	26.11	Basement	0	0	Spring					

Well no.	pH	EC	TDS	Cation (mg/l)				Anion (mg/l)			
		µS/cm	mg/l	Ca^{2+}	Mg^{2+}	Na^{+}	K^{+}	CO_3^{2-}	HCO_3^{-}	SO_4^{2-}	Cl^{-}
1	7.1	25,290	17,677	1500.0	727.18	3800	85	0.00	286.40	2811.4	8610.64
2	6.6	5710	3680	231.0	82.92	1020	36	0.00	30.50	482.5	1812.77
3	7.8	5610	3924	370.5	172.23	760	21	0.00	109.70	1160.4	1384.75
4	7.6	6830	4731	447.0	210.50	840	25	0.00	140.00	1451.12	1686.88
5	7.27	7670	4241	421.9	209.952	833.72	27.08	0.00	112.65	466.67	2225
6	8	12,048	7649	800.0	284.00	1449	30	0.00	210	1802	3179

D discharge, *PD* pumping duration, *T* transmissivity, *SD* saturated thickness, *HC* hydrlic conductivity, *h* hour

[a] Hydraulic parameters : obtained from Ismail (2009)

rest directly on the fractured basement rocks upstream of the wadies or they cap the sedimentary rocks in the downstream portion. Groundwater occurs under free water table conditions. The total depth of these shallow wells ranges from 3 to 7.5 m, while the depth to water table ranges between 1.5 and 5.2 m. The main source of recharge is local rainfall, flash surface runoff, as well as the possibility of upward leakage from the deep aquifers through fault planes. This aquifer is considered of limited use due to its limited extension, small thickness and high salinity of its groundwater (TDS between 3680 to 17,677 mg/l).

Oligocene sandstone aquifer (El Nakhil Formation)

The Oligocene sandstone is detected as a water-bearing formation in the Wadi El Nakhil sub-basin. This aquifer is tested to be productive downstream of this wadi at two wells which have total depths of 157 and 166 m. The static water table depth varies from 17 to 17.5 m. The Oligocene groundwater is mainly brackish and TDS ranges between 4241 and 4731 mg/l. The values of the hydrologic parameters of wells 5 and 6 (discharge rate 65.5 and 69 m^3/hour, transmissivity 1098.8 and 863.3 m^2/day, and hydraulic conductivity 7.79 and 5.82 m/day, Ismail 2009) respectively, indicate a good potential for the investigated aquifer.

Pre-Cambrian fractured basement aquifer

The fractured basement rocks constitute the majority of the catchment area to the west. The groundwater occurs under free water table conditions. The meta-volcanic rocks are known to be a water-bearing formation through one natural spring (Ain Al-Ghazal). The basement rocks at this site are impermeable, but they are dissected by fractures and joints which act as good conduits for water. Although the basement rocks are directly recharged from the local precipitation, the water is saline (TDS 17,677 mg/l) due to evaporation processes.

Geophysical data

The previous results (obtained from different sources) of the qualitative and quantitative interpretation of 32 vertical electrical soundings, in addition to four land magnetic profiles of total magnetic field intensity, led to delineate the groundwater occurrence along the main channels and some tributaries (Fig. 6). Water bearing formations, zones and different types of aquifers were defined as both semi-confined and water table aquifers. The water bearing formations are Quaternary alluvial deposits, the Oligocene sandstone of El Nakhil Formation, the Nubian sandstone and the fractured Pre-Cambrian basement rocks. The hydrogeological evaluation of the detected aquifers in the

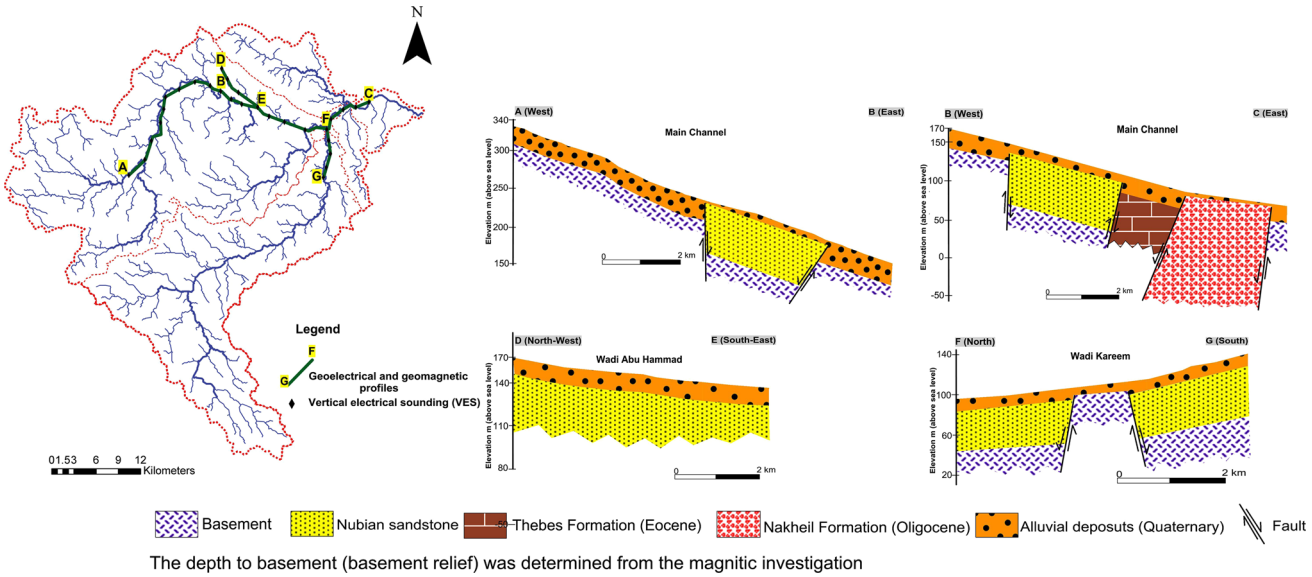

Fig. 6 Subsurface data of the study area based on the vertical electrical soundings, and land magnetic profiles (completed from Khaled 2002, 2007)

study area indicates a moderate groundwater potential. The data show the heterogeneity of subsurface where the structural setting plays an important role in the occurrence of groundwater. The uplifting of basement rocks has decreased the thickness of the sedimentary cover and hence reduces the potential for finding groundwater resources.

In addition to the summarized data in Fig. (6), the Red Sea governorate project (the frame of development of Bedouin communities, 2007) has completed geophysical explorations which have been carried out to detect the depths and the extended water-bearing formations along the main course of El Nakhil sub-basin. The results indicate that the depth of water-bearing formations in the middle portion of the main channel of the El Nakhil sub-basin is deeper than its upstream portions. The depth of the upper surface of the water-bearing formation in the middle portion varies from 65 m to 70 m from the ground surface, while it ranges between 30 m and 60 m in the northern and southern portions. This graben basin could be attributed to the impact of the structural setting. The drilled wells (nos. 4 and 5) in the downstream portions reveal that the saturated zone is thicker, from 139.9 to 148.2 m.

Rainfall analyses and surface runoff estimation

Analyses of the daily precipitation in the study area over the years 1985–2014 reveal that the rainy season is usually from September to March. The average annual rainfall during this period reaches up to 3.5 mm. The visualization and analysis of monthly TRMM data (1998–2015), as well as the analyses of annual long-term rainfall data (1945–2010) indicate that the study area is subject to sudden rainfall events (Fig. 7 a&b). From the daily records, 12 single events were documented (Table 1), where the maximum value reached 27 mm (22/3/1991). These events often generate surface runoff, turn into floods and represent a risk to the region (Fig. 7c, d). The mentioned maximum daily value has been used in the subsequent calculations of the surface runoff.

In the present study, the estimation of surface runoff (Q) is based on the curve number method using Eqs. 5, 6, and 7. The studied sub-basins have more curve number values; therefore Eq. (7) was used to calculate the weighted mean curve number for these sub-basins. The weighted curve number values for soil group (A), and two types of land covers; Desert shrubs (<30 % ground cover, litter, grass, and brush), and Fallow Bare soil, were used. The results (Table 3) reveal that the studied sub-basins have actual runoff (Q) ranging between 1.90 mm and 2.25 mm from a single event of 27 mm. The total runoff volume for this event (Qv) in an area "A" was calculated using Eq. (8), and ranges between 70.47×10^3 m^3 (Wadi Byada sub-basin) and 1723.33×10^3 m^3 (Wadi Abu Hammad sub-basin). The summation of the surface runoff volume for El Ambagi basin (total area 1529.60 km^2) is 3316.42×10^3 m^3. Evaluation of these results reflects that the sub-basins can receive runoff ranging between 7.05 and 8.33 % of a single rainfall event of 27 mm. The remaining rainfall is mainly lost by infiltration. In modeling single floods, the effects of evapotranspiration are ignored (Ramirez 2000) because its magnitude during the time period in which the flood develops is negligible.

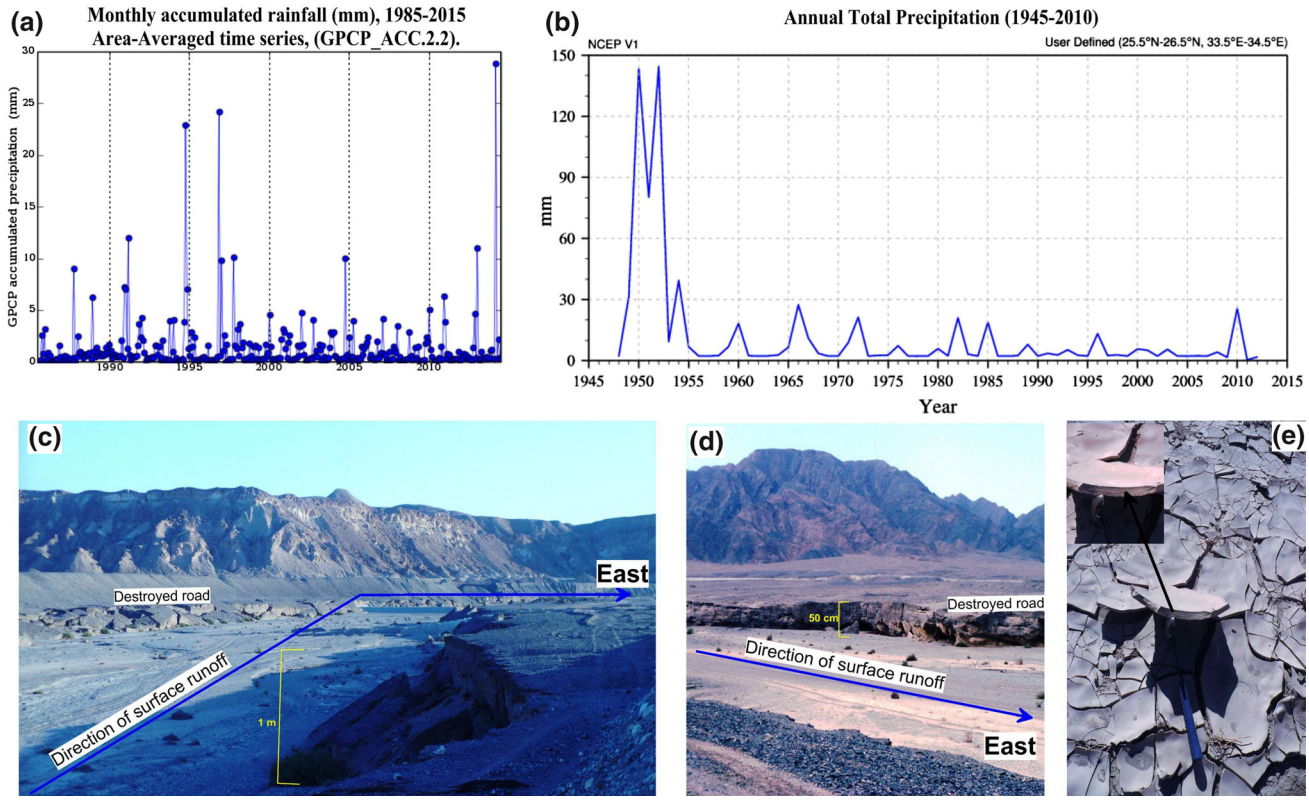

Fig. 7 Rainfall events and their hazard in the study area. **a** Precipitation data estimated from satellite, TRMM (Monthly accumulated rainfall). **b** Annual total precipitation as a consequence of the climatic change affecting the area. **c** and **d** Field photos showing the effects of flash floods (January 2015). **e** Mud cracks (ca. 5 cm thick) formed as a result of the last rainfall event in January 2015

Table 3 Results for estimation of surface runoff using curve number method

Input				Output			Evaluation of the outputs	
Sub-basins	Total area (A) km^2	Weighted (CN)	Maximum daily Precipitation (P) mm	Potential Maximum Retention (S)	Initial Abstraction (Ia) mm	Runoff volume (Q) mm	Total Runoff volume (Qv) (m^3) × 10^3	Runoff (Q) to rainfall (P) Q/P (%)
Wadi Bayda	37.00	78	27	71.64	14.33	1.90	70.47	7.05
Wadi El Nakhil	110.43	78		71.64	14.33	1.90	210.31	7.05
Wadi Kareem	564.20	79		67.52	13.50	2.25	1268.50	8.33
Wadi Abu Hammad	766.50	79		67.52	13.50	2.25	1723.33	8.33
Others	51.47	74		89.24	17.85	0.85	43.81	3.15
El Ambagi basin	1529.60						3316.42	

The curve numbers are the weighted values for soil group (A), and land cover of desert shrubs (<30 % ground cover, litter, grass, and brush overstory), and Fallow bare soil, soil group (A): sand, loamy sand and sandy loam

Morphometric analyses

The results from DEM analyses reveal that the study area contains four sub-basins which have intensive drainage networks (Fig. 8). These sub-basins have areas between 37 km^2 (Wadi Bayda) and 766.50 km^2 (Wadi Abu Hammad). The morphometric parameters (Table 4) of these sub-basins have been computed and summarized as follows (Table 5):

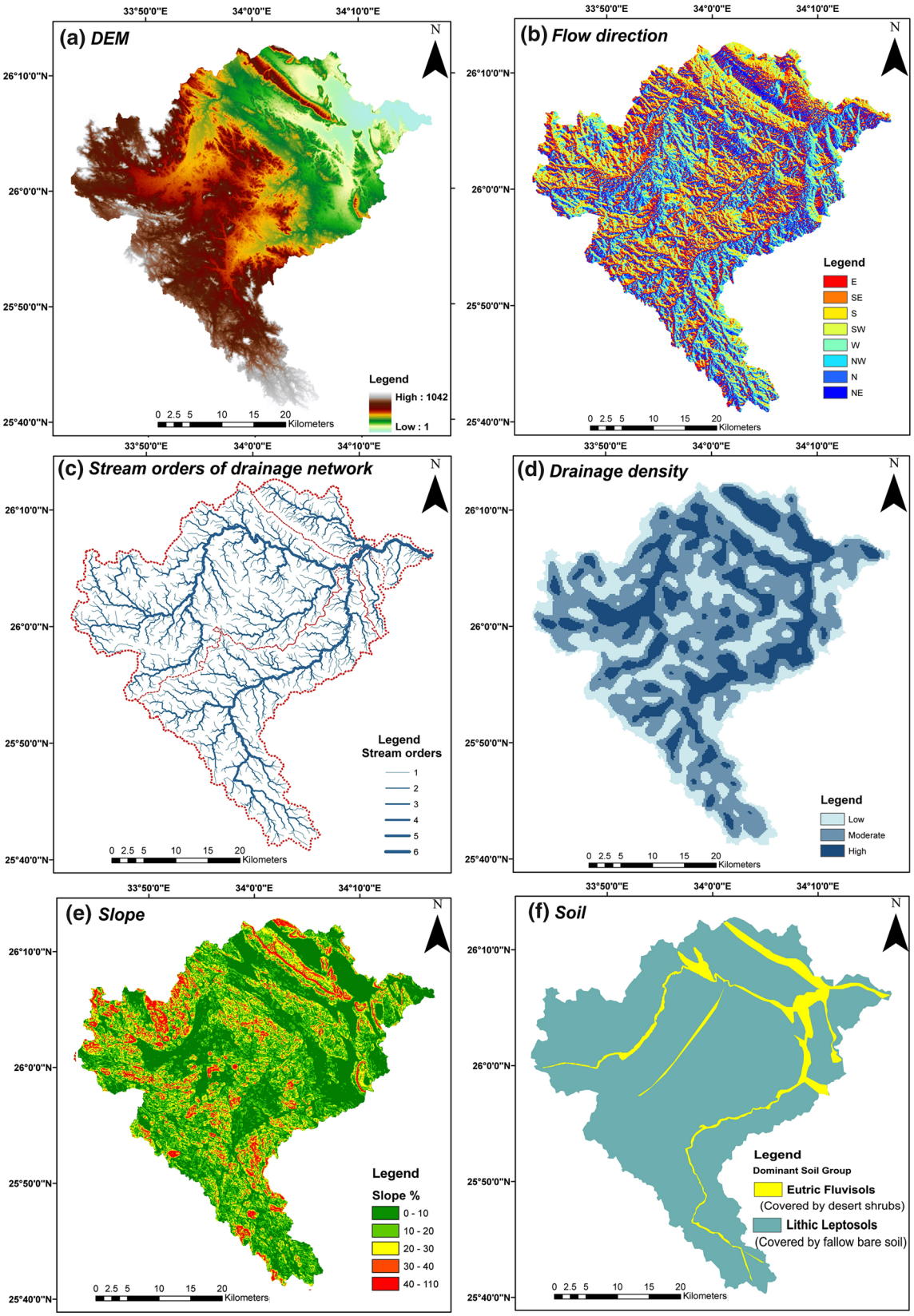

Fig. 8 Different data layers used in the assessment of water resources. **a** DEM **b** Flow direction **c** drainage network with its stream orders **d** drainage frequency **e** Slope of the study area **f** Soil map

Table 4 Methodology adopted for computation of the morphometric parameters

Serial number	Morphometric parameters	Units	Methods	References
Linear				
1	Stream order (u)		Hierarchical order, DEM analyses by Arc GIS	Strahler (1964)
	Sum of all stream numbers (SN_u)		Counted from analysis, (N_u is the number of order u)	
2	Stream length (L_u)	km	DEM analyses by Arc GIS	Horton (1945)
	Sum of all stream lengths (SL_u)	km	DEM analyses by Arc GIS	–
3	Length of main channel (L_m)	km	Measured through Arc GIS	–
4	Order of the main channel (K)		Identified from analysis	–
5	Bifurcation ratio (Rb)		$Rb = N_u/N_{u+1}$	Horton (1945)
6	Weighted mean bifurcation ratio (WMRb)		$WMRb = Sum\{(Rb\ u/u + 1) \times (N_u + N_{u+1})\}/SumN$	Strahler (1953)
7	Sinuosity (Si)		Si = Lm/Lb	Gregory and Walling (1973)
Relief				
8	Relief (R)	*M*	Calculated from DEM analyses	
9	Relief ratio (R_r)		Rr = R/Lb (Schumm, 1956)	Schumm (1956)
10	Ruggedness number (R_n)		Rn = D × R	Melton (1957)
Areal				
11	Area (A)	km^2	Measured through Arc GIS	
12	Perimeter (P)	km	Measured through Arc GIS	
13	Basin length (Lb)	km	Measured through Arc GIS	
14	Drainage density (D)	km^{-1}	D = SLu/A (Horton, 1945)	Horton (1945)
15	Stream frequency (F)	km^{-2}	F = SNu/A (Horton, 1945)	Horton (1945)
16	Circulatory ratio (Rc)		$Rc = 4\pi A/P^2$	Miller (1953)
17	Elongation ratio (Re)		$Re = 2(A/\pi)^{0.5}/Lb$ (Schumm, 1956)	Schumm (1956)
18	Length of overland flow (Lo)	km	Lo = 1/(2D)	Horton (1945)
19	Drainage texture (Rt)		$Rt = SN_u/P$	Horton (1945)
20	Texture ratio (T)		$T = SN_1/P$ where SN_1 is total number of 1st order streams	Horton (1945)
21	Form factor (Rf)		$Rf = A/Lb^2$	Horton ((1932)
22	Basin shape index (Ish)		$Ish = 1.27.\ A/Lb^2$	Hagget (1956)

Stream orders (N_u) and stream length (L_u)

Most of the drainage basins are of the 4th and 5th stream orders, only the Wadi Bayda sub-basin is 3rd order. A dendritic drainage pattern was noted in the surface of tableland areas, indicating the homogeneity in rocks and lack of structural control. The total stream lengths range between 38.5 and 903.88 km. The stream length is hence an indicator of the relation between climate, vegetation, and resistance of rocks and soils to erosion.

Bifurcation ratio (R_b) and sinuosity (Si)

The Bifurcation Ratio is not the same from one order to the next, therefore it has been expressed by its weighted mean value. Values of the weighted mean bifurcation ratio range between 3.84 and 5. These values are relatively high (greater than 3), which indicates a structural control in the drainage development. On the other hand, the obtained sinuosity values are more than unity.

Relief (R), relief ratio (R_r) and ruggedness number (R_n)

The elevation difference between the highest and lowest points of the watershed is its total relief, whereas relief ratio is the total relief of the watershed divided by the maximum length of the watershed. The obtained values of the total relief range between 176 and 860 m. The relief measures the overall steepness of a watershed, and is an indicator of the erosion processes operating on the slope of a watershed. The relief ratio normally increases with decreasing watershed areas. It is noticed that the relief ratio values are small (range between 0.01 and 0.03), indicating generally gentle slopes in the studied sub-basins. The area

Table 5 Results of morphometric analysis and the hazard degrees of the effective parameters of the studied sub-basins

Serial number	Morphometric parameters		Sub-basins					El Ambagi Basin
			Bayda	El Nakhil	Kareem	Abu Hammad	Others	
1	Linear	Sum of stream numbers (SN_u)	34.00	94.00	403.00	537.00	38.00	1106.00
2		Sum of stream lengths (SL_u)	38.50	148.72	707.44	903.88	66.53	1865.07
3		Length of main channel (Lm)	15.60	22.50	65.00	62.00	18.67	76.00
4		Order of the main channel (K)	3.00	4.00	5.00	5.00	6.00	6.00
5		Bifurcation ratio (Rb)	5.35	4.38	4.30	4.54	7.00	4.04
6		Weighted mean bifurcation ratio (WMRb)	4.35	4.10	3.94	4.20	5.00	4.26
7		Sinuosity (Si)	1.11	1.26	1.08	1.09	1.44	1.09
8	Relief	Relief (R)	178.00	520.00	601.00	860.00	122.00	1041.00
9		Relief ratio (Rr)	0.01	0.03	0.01	0.02	0.01	0.01
10		Ruggedness number (Rn)	0.19	0.70	0.75	1.01	0.16	1.27
11	Areal	Area (A)	37.00	110.43	564.20	766.50	51.47	1529.60
12		Perimeter (P)	40.00	56.51	183.25	169.00	27.00	260.71
13		Basin length (Lb)	14.00	17.90	60.00	57.00	13.00	70.00
14		Drainage density (D)	1.04	1.35	1.25	1.18	1.29	1.22
15		Stream frequency (F)	0.92	0.85	0.71	0.70	0.74	0.72
16		Circulatory ratio (Rc)	0.29	0.43	0.21	0.34	0.88	0.28
17		Elongation ratio (Re)	0.50	0.66	0.50	0.55	0.62	0.63
18		Length of overland flow (Lo)	0.48	0.37	0.40	0.42	0.39	0.41
19		Drainage Texture (Rt)	0.85	1.66	2.20	3.18	1.41	4.24
20		Texture ratio (T)	0.65	1.24	1.64	2.47	1.22	3.24
21		Form Factor (Rf)	0.19	0.34	0.16	0.24	0.30	0.31
22		Basin shape index (Ish)	0.24	0.44	0.20	0.30	0.39	0.40

The hazard degree of the studied sub-basins

Relation with hazard	The effective morphometric parameters	Minimum and maximum values of the parameter in all sub-basins		Weight of the parameters which affected the hazard degree			
				Sub-basins			
		X_{min}	X_{max}	Bayda	El Nakhil	Kareem	Abu Hammad
Proportional	Area (A)	37.00	766.50	1.00	1.40	3.89	5.00
	Drainage density (D)	1.04	1.35	1.00	5.00	3.79	2.81
	Stream frequency (F)	0.70	0.92	5.00	3.76	1.25	1.00
	Basin shape index (Ish)	0.20	0.44	1.68	5.00	1.00	2.69
	Relief ratio (Rr)	0.01	0.03	1.57	5.00	1.00	2.07
	Ruggedness number (Rn)	0.19	1.01	1.00	3.49	3.74	5.00
	Drainage texture (Rt)	0.85	3.18	1.00	2.40	3.32	5.00
Inverse	Weighted mean Rb (WMRb)	3.94	4.35	1.00	3.44	5.00	2.46
	Length of overland flow (Lo)	0.37	0.48	1.00	5.00	3.99	3.07
	Sinuosity (Si)	1.08	1.26	4.29	1.00	5.00	4.90
Summation of hazard degree				18.54	35.48	31.98	33.99
Classification of the sub-basins (hazard degree)				1	5	4	5
				Low hazard	High hazard	Medium hazard	High hazard

under investigation is characterized by medium relief. The ruggedness number reflects the structural complexity of the terrain. The obtained high values (ranging between 0.19 and 1.01) indicate high impacts of erosion process.

Drainage density (D) and stream frequency (F)

Drainage density reflects the closeness of channel spacing, thus providing a quantitative measure of the average length

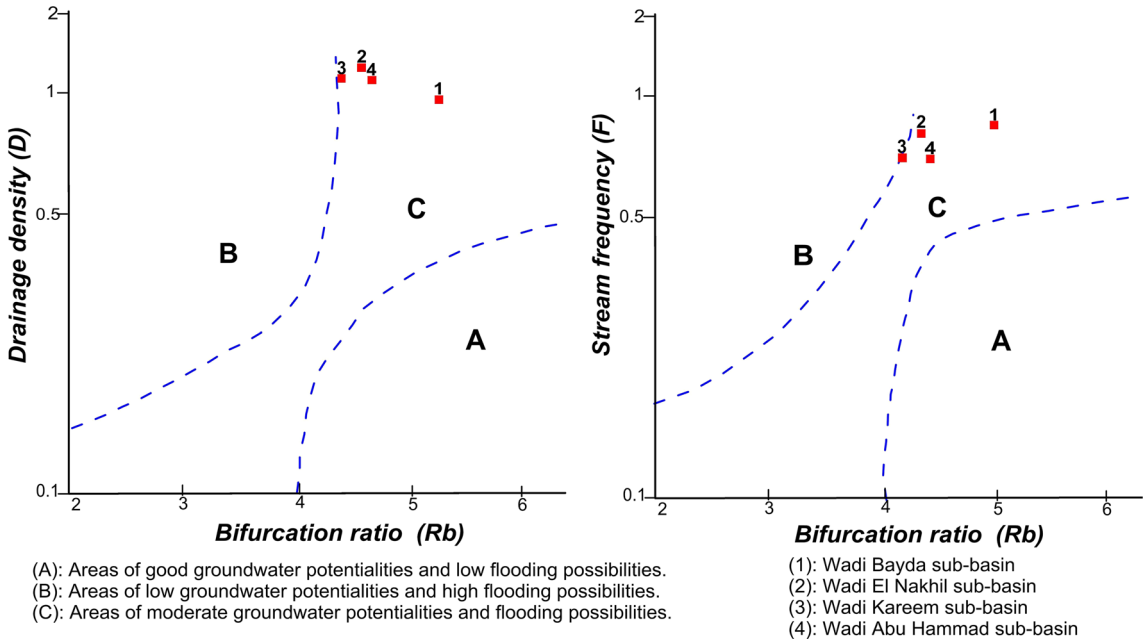

Fig. 9 Relationships of bifurcation ratio (R_b) versus drainage density (D) and bifurcation ratio versus stream frequency (F), (curves after El Shamy 1992)

of stream channels for a whole basin. It is also an indicator of drainage efficiency of the watershed. The obtained values range between 1.04 and 1.35 km^{-1}. These values are comparably high and are developed in the regions of weak or impermeable subsurface material, sparse vegetation, and mountainous relief. On the other hand, the values of stream frequency are low (ranging between 0.70 and 0.92 km^{-2}), providing more possibilities for infiltration and groundwater recharge.

Based on EL Shamy (1992), the quantitative hydrogeomorphometric analysis revealed that all sub-basins occupy domain (zone C), pointing to moderate groundwater potential and probability for flooding (Fig. 9). The severe floods along the main channels are mostly due to the cumulative impact of these moderate floods.

Circularity ratio (R_c) and elongation ratio (R_e)

The circularity ratios for all sub-basins are less than 0.5. Therefore, they have an elongated shape which allows slow disposal of water, and results in a broad and low-peaked hydrograph. Therefore, the reduction of runoff velocity can be achieved by providing water harvesting structures, like dams and surface reservoirs. The elongation ratios confirm the values of Rc where all parameters are more than 0.5, showing elongated basins. This suggests that the studied sub-basins have opportunities for both groundwater recharging through infiltration process and occurrence of surface runoff.

Length of overland flow (L_o), drainage texture (R_t) and basin shape index (Ish)

The length of overland flow is the length of the water flow path over the ground before it gets concentrated into definite stream channels. It ranges between 0.37 (Wadi El Nakhil) and 0.48 (Wadi Bayda). These values reflect that Wadi El Nakhil provides the fastest surface water concentration while Wadi Bayda shows the slowest. The drainage texture values in the studied sub-basins are less than 6.4 km^{-1}, therefore they can be classified as a coarse texture (Smith 1958). This classification pointed out that the drainage texture ratio depends upon a number of natural factors such as climate, rainfall, vegetation, rock and soil type, infiltration capacity, and relief. The soft or weak rocks unprotected by vegetation produce a fine texture, whereas massive and resistant rocks cause coarse texture. The basin shape index describes the relation between the area and the length of the basin. The studied sub-basins have shape index values ranging between as 0.24 and 0.44. These values indicate an elongated basin network and in turn suggest a good chance for groundwater recharge.

Assessment of flash flood hazard of the studied basins

The hazard degrees for the selected ten parameters were obtained according to Eqs. 2 and 3, and the results are shown in Table 5. The studied sub-basins have hazard degrees ranging between 18.54 (Wadi Bayda) and 35.48

(Wadi El Nakhil). Accordingly, these sub-basins were classified into three groups:

- Basins with high flash flood hazard: Wadi El Nakhil and Wadi Abu Hammad sub-basins.
- Basins with medium flash flood hazard: Wadi Kareem sub-basin.
- Basins with low flood hazard: Wadi Bayda sub-basin.

Flow direction, slope, and soil characters

Flow direction, slope and soil are important layers in the assessment of water resources because they provide data about the surface of the study area and the nature of the stream flow (Fig. 8). The flow direction layer reflects that the surface water runs with the general slope with few exceptions where some local mountains direct the surface water to the lower areas. The general flow directions of the main channels of the sub-basins are directed towards the east (20 %), while the other tributaries have flow directions towards the north (18 %) and northeast (13 %). Most of the study area has slope values between 10 % (floor of the sub-basins) and 30 %, (watershed areas). On the other hand, the upper parts of the tableland and the Red Sea terrains have slope values exceeding 40 %. This is a result of the relief difference where these parts are occupied by the basement mountains which act locally as recharge areas. The prepared soil map of the study area (Fig. 6c) shows that the studied basin contains two main types of soils. The first type are the Eutric Fluvisols composed of sand and loamy sand, located in the floor of the sub-basins and along the tributaries. The second type is Lithic Liptosols represented by fallow bare soils which cover the stony mountainous area. The sandy loamy soil has a moderate infiltration capacity and is classified as a moderately to well-drained soil.

Discussion

El Ambagi basin represents a typical area with hyper-arid conditions. Although this basin falls into an arid zone environment, it receives certain amounts of annual rainfall which provide the opportunity for surface runoff and also for groundwater recharge. The highlands represent the main recharge area while the lowlands act as water storage/discharge areas. The obtained results show that the study basin has potential for both groundwater and surface water exploitation.

Groundwater resources

The area under consideration is covered by a variety of igneous, metamorphic and sedimentary rocks belonging to Pre-Cambrian and Phanerozoic ages. Special focus is placed on the exposures of Nubian and Oligocene sandstones because these sediments have relatively high porosities. Also, they were rarely explored (only 2 wells in Oligocene rocks groundwater aquifer). On the other hand, the Nubian sandstone is the most important aquifer which can be considered a key water resource within Egypt, and large quantities of groundwater are presently available (Voss and Soliman 2014). The measured effective porosity and permeability revealed a high potential of the Nubian sandstone and the Oligocene formations. This result was confirmed by the petrographic investigations. The facies distribution and microfacies examination show that these sandstones are fluvial-marine sediments which were affected by many diageneses processes, which have led to increased porosity and permeability. Structurally, the area is characterized by a complicated structural setting of fractures having different types and magnitudes. Gebel Duwi district represents a syncline whose axial line lies roughly along the central part of Wadi Nakhil (Youssef 1957). Many faults are also recorded at the contact between the Nubian sandstone and the basement rocks. The interpretation of the satellite imagery revealed many regional fracture lineaments, some of which affect the Tertiary sedimentary rocks and very few others affect the Quaternary deposits in the study area. The eastern part of the studied basin seems to have a moderate number of lineaments, probably as a consequence of the soft rocks of Mesozoic and Cenozoic rocks. Moreover, the intensity of tectonic movements in the area also decreases westwards, away from the basement complex. The concentration of linear features decreases from the center of study area to both the northeast and southwest. This may be attributed to the tectonic movements occurring during the Oligo-Miocene which were accompanied by the rifting of the Red Sea graben (Said 1992). The analysis of these fracture lineaments reveals that the most intensive anomaly has been concentrated on the middle part of the studied basin. The water bearing formations in the intermountain basins store considerable amounts of fossil water (nonrenewable) that is believed to have been recharged during previous wet climatic periods (Sturchio et al. 2004; Sultan et al. 2011). It is possible that structural lineaments in this area cause localized recharge conditions for the groundwater aquifer. This fact was confirmed by the isotope analyses which were carried out by Amer et al. (2013). A portion of the rainwater is thought to infiltrate through joints and faults and recharge the Oligocene sandstone, Nubian sandstone, and basement rocks. This also corresponds with what was stated by Sultan et al. (2000) where chemical and isotopic analysis of the groundwater in the Eastern Desert showed that infiltration into the shallow alluvial aquifers was derived mainly from regional precipitation and flash floods.

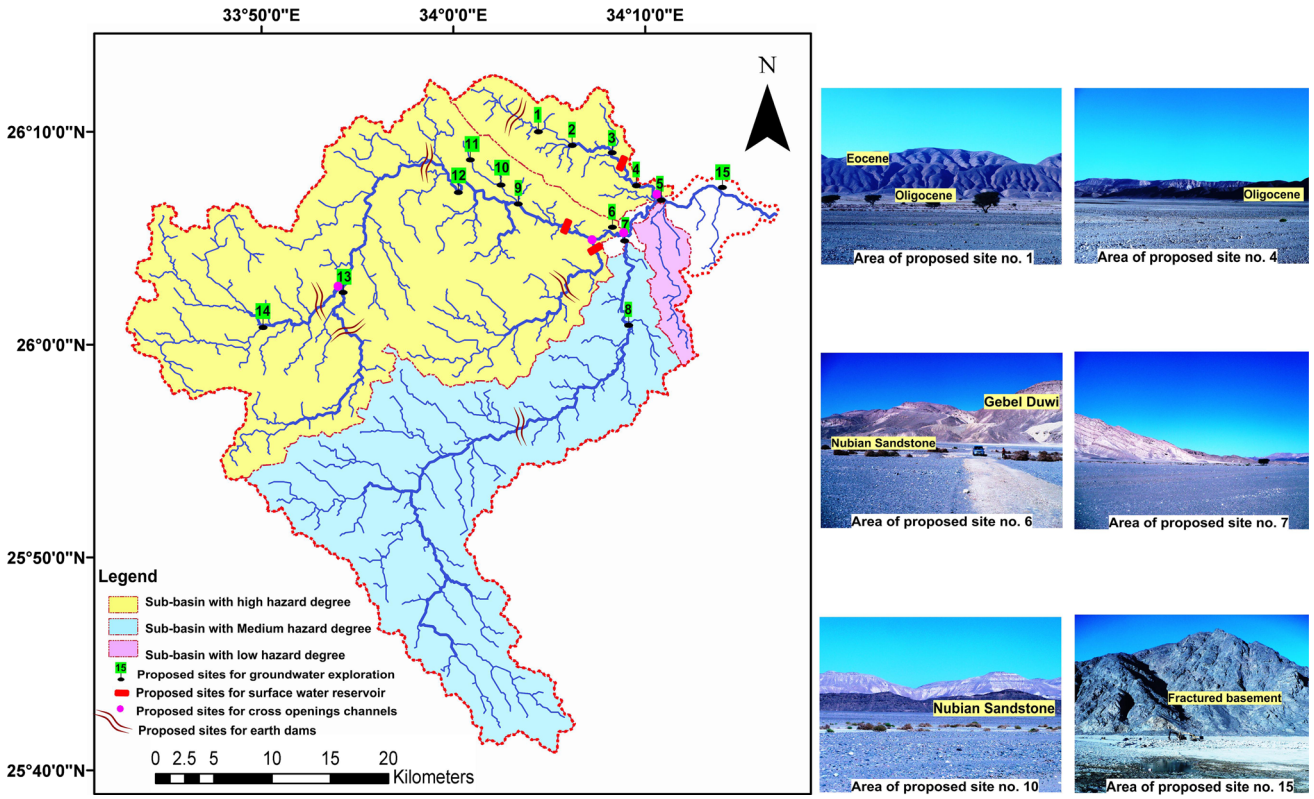

Fig. 10 Recommendation map pointing out the hazard classification of the studied sub-basins, and proposed sites for groundwater and surface water development; photos showing some of the proposed sites (1, 4, 6, 7, 10, and 15) which have been verified in the field

The available geophysical data indicate the Oligocene and Nubian sandstones as well as the basement rocks are saturated. Also, the obtained values of the morphometric parameters indicate that the study area has a potential for recharge of groundwater. This corresponds to the results of Abdalla (2012) in a basin from the Central Eastern Desert where the Quaternary deposits, in addition to the fractured Precambrian basement rocks were identified as very good to good prospecting zones. Moreover, the thick fluvial deposits of old drainage systems which received much surface water in the past pluvial periods still store the ''fossil'' groundwater.

This also was confirmed through quantitative hydro-geomorphometric analysis which pointed out that the studied sub-basins have moderate groundwater potential and probability of flooding (Fig. 9). The investigation of the basin indicates that several specific sites have favorable conditions for groundwater reservoirs and should be subjected to exploration (Fig. 10). The selected sites for groundwater exploration have more intense structural lineaments, low slopes, and represent the downstream and middle parts of the drainage basins. These conditions present opportunity for recharge of the aquifers through the fractured zones. The drilling in sites located along the fractures showed that these fracture zones can receive increased amount of recent recharge through rainfall, and accordingly, decrease the groundwater salinity. All the selected sites were confirmed by both geophysical data and field verifications. Only three sites (nos. 13, 14 and 15) are recommended for exploration of the fractured basement while the other twelve sites are recommended for the explorations of Nubian sandstone and Oligocene sandstone (Table 6 and Fig. 10).

Surface water resources

Rainwater harvesting could be an efficient approach to harness the excess runoff, and hence can be used during deficit times. Rainwater harvesting is applicable to minimize water losses and to augment water supplies in watershed systems, in addition to avoiding the probability of flash flood and its hazard which can abort any development bases. The area along the Red Sea coast has frequently been affected by flash floods and mass deposition hazards and different types of infrastructure and urban areas have suffered property damage (Youssef et al. 2009). Meteorologically, the area is likely to be affected by strong thunderstorms, and it may face intense cloudbursts in the next few years (Zaid 2009). The obtained results reveal that the studied basin contains 4 sub-basins which have an

Table 6 Proposed sites for water resources protection and development

Groundwater exploration

Site	Coordinates		Target	Well type	Landforms	Lithology	Slope %	Soil	Structural lineaments		Drainage density	Elevation m (a.s.l)	Geophysical data
	Long. (E)	Lat. (N)							Density (km^{-1})	Frequency (km^{-2})			
1	34.06	26.17	Explore oligocene sandstone	Drilled	Lowlands (water collector)	Quaternary underlain by oligocene	0–10 (Gentle slope)	Eutric Fluvisols (Sandy loam and loamy sand)	0.7 (H)	0.22 (H)	1.35 (H)	167	Saturated thickness ~55 m
2	34.11	26.15							0.7 (H)	0.22 (H)	1.35 (H)	140	Saturated thickness ~70 m
3	34.14	26.15							0.7 (H)	0.22 (H)	1.35 (H)	113	
4	34.159	26.12							0.75 (H)	0.24 (H)	1.35 (H)	91	Saturated thickness 135 m
5	34.18	26.11							0.75 (H)	0.24 (H)	1.35 (H)	79	
6	34.14	26.09	Explore Nubian sandstone	Drilled	Lowlands (water collector)	Quaternary underlain by Nubian sandstone	0–10 (Gentle slope)	Eutric Fluvisols (Sandy loam and loamy sand)	0.7 (H)	0.2 (H)	1.18 (M)	149	Saturated thickness ~45 m
7	34.15	26.08							0.7 (H)	0.18 (M)	1.25 (H)	104	Saturated thickness ~50 m
8	34.15	26.014							0.65 (M)	0.18 (M)	1.25 (H)	161	
9	34.05	26.11							0.7 (H)	0.18 (M)	1.18 (M)	169	Saturated thickness ~40 m
10	34.04	26.12							0.7 (H)	0.18 (M)	1.18 (M)	184	
11	34.01	26.15							0.7 (H)	0.18 (M)	1.18 (M)	230	
12	34.00	26.12							0.7 (H)	0.18 (M)	1.18 (M)	220	Saturated thickness ~50 m
13	33.90	26.04	Explore basement	Hand dug	Lowlands (water collector)	Basement	0–10 (Gentle slope)	Fallow bare soil	0.7 (H)	0.18 (M)	1.18 (M)	340	No data, therefore, it is recommended to drill test wells
14	33.83	26.02							0.7 (H)	0.18 (M)	1.18 (M)	411	
15	34.23	26.12							0.8 (H)	0.26 (H)	1.29 (H)	53	

Surface water (protection and harvesting)

Site	Coordinates		Proposed structure	Sub-basins	Hazard degree	Landforms	Slope %	Soil	Drainage Density	Flow direction	Elevation m (a.s.l)	Target
	Long. (E)	Lat. (N)										
1	34.15	26.13	Surface water reservoir	El Nakhil	High	Main channels	0–10 (Gentle slope)	Eutric Fluvisols (Sandy loam and loamy sand with gravels)	1.35 (H)	Southeast	109	Freshwater storage (seasonal rainfall)
2	34.12	26.08		Abu Hammad	High				1.18 (M)	Northwest	125	
3	34.10	26.09		Abu Hammad	High				1.18 (M)	Southeast	131	
4	34.20	26.11	Cross openings channels	El Nakhil	High	Downstream portions of the drainage basins	0–10 (Gentle slope)	Eutric Fluvisols (Sandy loam and loamy sand with gravels)	1.35 (H)	Southeast	79	Protect the road from flash floods
5	34.15	26.08		Kareem	Medium				1.25 (H)	East	106	
6	34.12	26.08		Abu Hammad	High				1.18 (M)	East	122	
7	33.90	26.04		Abu Hammad	High				1.18 (M)	Northeast	338	

Table 6 continued

Surface water (protection and harvesting)													
Site	Coordinates		Proposed structure	Sub-basins	Hazard degree	Landforms	Slope %	Soil	Drainage Density	Flow direction	Elevation m (a.s.l)	Target	
	Long. (E)	Lat. (N)											
8	34.04	26.18	Earth dams	El Nakhil	High	Main channels	0–10 (Gentle slope)	Eutric Fluvisols (Sandy loam and loamy sand)	1.35 (H)	Southeast	180	Decreasing the flood speed, provide chances for groundwater recharge, and save the soil from erosion	
9	34.06	25.93		Kareem	Medium				1.25 (H)	East	310		
10	33.98	26.14		Abu Hammad	High				1.18 (M)	Southeast	247		
11	33.90	26.03		Abu Hammad	High				1.18 (M)	Northeast	360		
12	33.90	26.02		Abu Hammad	High				1.18 (M)	North	378		
13	34.10	26.04		Abu Hammad	High				1.18 (M)	Northeast	203		

H high, *M* moderate as l above sea level

intensive drainage network. Although the area of study has a gentle slope over most of its surface, the analyses of the precipitation data confirm that some events were characterized by a sudden increase in the amount of rainfall. This has to be considered in flood scenarios, where the studied basin drainage flows to the tourist city of El Quseir. Two of the investigated sub-basins show high hazard degrees (Table 5) and have therefore to be protected to avoid flash floods. In this regard, the values of the actual runoff (runoff depth) and the total runoff volume of the studied sub-basins can contribute significantly to the evaluation of the rainwater harvesting potential and to evaluating the flash flood hazard. The estimated runoff volume from a single rainfall event of 27 mm reaches 3316.42 x 10^3 m^3. The runoff varies between 10 % and 15.3 % of the average rainfall amount. The main road (El Quseir-Qena, Fig. 1) is subjecting to destruction as a result to any flash floods (Figs. 7 c, d). The road was established along the main channel of El Ambagi basin, and extended along the floor of the basin, so it works as water collector from the whole catchments. Therefore it is protection becomes necessary. Most of the surface runoff runs to the east in ephemeral drainage towards the coastal plain, or to the sea. Therefore, it is recommended that further construction of surface reservoirs and different types of dams should be applied. This infrastructure will provide fresh drinking water and will also serve to control flash floods. Such techniques of water conservation are very suitable for local inhabitants to keep the sort of settlement in the study area (such as the main road and Qusier City). The present study introduces some recommendations for future surface water development in the form of suggested sites for surface reservoirs and dams to conserve large quantities of surface water. From this point of view, harvesting the overland flow or lost runoff water from the promising drainage basins by implementing commonly used structures such as percolation tanks, check dams and subsurface dams is of utmost necessity (Elewa and Qaddah 2011). The following recommendations should be taken into consideration for harvesting and managing of the surface water as well as to avoid future risk of flash floods (Table 6) and (Fig. 10):

a) Surface water reservoirs should be constructed at the recommended sites (Fig. 10) to store large amount of surface water (ranging from 3000 to 5000 m^3). **b)** Alternative earth dikes should be established along the drainage lines in the upstream portions of basins. These dykes will serve for dispersing the main runoff and hence mitigating flood flash in the case of Wadi El Nakhil abd Wadi Abu Hammad sub-basins (high hazard degree). On the other hand, these dikes can also increase groundwater recharge.

c) Cross open channels should be established under the main road to provide a passage for water flow to avoid seasonal road damage.

Conclusions

Arid regions are highly vulnerable to environmental and particularly hydrological changes. Data scarcity for most of such areas along the Red Sea coast and the Eastern Desert of Egypt is a great challenge for water resources assessment at practical scales. The El Ambagi basin is one of these regions with scarce or missing hydrological and hydrogeological data. The current research addresses these challenges by the use of basic geological studies, integration of remote sensing and GIS, and field investigations. This area has a lack of water for mining and drinking purposes. In this study, an attempt is made to define a scientific approach for identifying the most appropriate sites for groundwater exploration and surface water management. This approach is based on the GIS data layers which include DEM, landforms, geologic setting, watershed areas, rainfall analyses, drainage lines, morphometric parameters, flow direction, slope, soil, surface runoff, structural lineaments and geophysical data. It also includes a verification of the site suitability through field investigations. This research has succeeded in providing information concerning the exploration of the Nubian sandstone and the Oligocene aquifers. Also, it focuses on the probability of flash floods and hazards which can hinder any development. The study has also pointed out that flood hazard evaluation is important for catchment management and especially for the sustainable development of the region's water resources. In the case of the lack of data and due to the fact that the flood assessment is dependent on the physiographic features of the basins, the flash flood hazard classification can be carried out on the basis of the effective morphometric parameters of the basins. It can be concluded that the current study represents an approach to integrate geo-informatics and geological investigations to assess the potential of water resources in arid, remote and data-scarce areas. It was shown that remote sensing and GIS can provide an appropriate platform for convergence of different data obtained from multidisciplinary research as well as from field investigation. We believe that the presented scientific approach is transferable to other arid areas with comparable conditions.

Acknowledgments Authors are thankful to the Ministry of Education, Youth and Sports of the Czech Republic and the Ministry of Higher Education of Egypt who funded the postdoctoral scholarship of the first author.

References

Abdalla F (2012) Mapping of groundwater prospective zones using remote sensing and GIS techniques: a case study from the Central Eastern Desert Egypt. J Afr Earth Sc 70:8–17

Allen RG, Pereira LS, Raes D, Smith M (1998). Crop evapotranspiration—guidelines for computing crop water requirements. FAO Irrigation and Drainage Paper, No. 56, FAO, Rome

Amer R, Sultan M, Ripperdan R, Ghulam A, Kusky T (2013) An integrated approach for groundwater potential zoning in shallow fracture zone aquifers. Int J Remote Sens 34(19):6539–6561

Bajabaa S, Masoud M, Al-Amri N (2013) Flash flood hazard mapping based on quantitative hydrology, geomorphology and GIS techniques (case study of Wadi Al Lith. Arab J. Geosci, Saudi Arabia). doi:10.1007/s12517-013-0941-2

Clarke J (1966) Morphometry from maps, essays in geomorphology. Elsevier Publication, New York

Conoco (1987) Geological map of Egypt, scale 1:500,000 GPC, Quseir Sheet

Davis JC (1975) Statics and data analysis in geology. Wiley, New York

El Bastawesy M (2007) Influence of DEM source and resolution on the hydrographical simulation of Wadi Keed catchment, Southern Sinai, Egypt. Egypt J Remote Sens Space Sci 9:68–79

El Bastawesy M, White KH, Nassr AH (2009) Integration of remote sensing and GIS for modeling flash floods in Wadi Hudain catchment Egypt. Hydrol Process 23(9):1359–1368

El Baz F (1995) Utilizing satellite images for groundwater exploration in fracture zone aquifers. In Proceedings of the International conference on water resources management in arid countries 1995, Oman. 2:419–427

El Baz F, Kusky TM, Himida I, Abdel Mogheeth S (1998) Ground water potential of the Sinai Peninsula, Egypt, 219. Desert Research Center, Cairo

EL Shamy IZ (1992) Towards the water management in Sinai Peninsula. Proc. 3rd Conference Geol. Sinai Development, Ismailia, 63–70

El Shazly EM, Abdel Hady M, El Ghawaby M, Salman A, El Kassas I et al (1981) New geological structural lineaments and drainage maps of Egypt, based on landsat imagery interpretation and field investigations. International symposium on remote sensing of environments, Cairo

Elewa HH, Qaddah AA (2011) Groundwater potentiality mapping in the Sinai Peninsula, Egypt, using remote sensing and GIS-watershed-based modeling. Hydrogeol J 19:613–628

El-Raey M (1998) Framework of integrated coastal area management of the Fuka-Matrouh area, Egypt, PAP/RAC-37-1995

Embarger L (1955) Afrique du Nord-Ouest. In: Plant ecology: reviews of research (ed.UNESCO), Paris, France: UNESCO. 219–249

Farr TG, Kobrick M (2000) Shuttle Radar Topography Mission produces a wealth of data. Amer Geophys Union Eos 81:583–585

Flügel E (1982) Microfacies analysis of limestone. Springer-Verlag, Berlin-Heidelberg-New York

Foody G, Ghoneim E, Arnell N (2004) Predicting locations sensitive to flash flooding in an arid environment. J Hydrol 292:48–58

Ghoneim E, El Baz F (2007) Dem-optical-radar data integration for paleo-hydrological mapping in the northern Darfur, Sudan: implication for groundwater exploration. Int J Remote Sens 28(22):5001–5018

Gregory KJ, Walling DE (1973) Drainage basin form and process. John Wiley and Sons, New York

Gupta RP (2003) Remote sensing geology. Springer, Heidelberg

Hagget P (1956) Locational analysis in human geography. Edward Arnold Ltd, London

Hamdan G (1980) The personality of Egypt (in Arabic), vol 1. Aalam El-Kotob, Cairo

Harmonized World Soil Database (2009) prepared by Food and Agriculture Organization of the United Nations, FAO/IIASA/ISRIC/ISS-CAS/JRC, 2009. Harmonized World Soil Database

(version 1.2). FAO, Rome, Italy and IIASA, Laxenburg, Austria. Available online: http://webarchive.iiasa.ac.at/Research/LUC/External-World-soil-database/HTML/index.html?sb=1

Horton RE (1932) Drainage basin characteristics transactions. Ame Geophys Union 13:350–361

Horton RE (1945) Erosional development of stream and their drainage basins. Geol Soc American Bull. 56:275–330

Ismail YL (2009) Hydrologic evaluation of Wadi EL Nakheil, Quseir Area, Eastern Desert, Egypt. In: 16th Symposium of Phanerozoic and Development in Egypt. Faculty of Science, AL Azhr University. pp. 1–14

Khaled MA (2002) Geophysical study on the groundwater occurrence in Wadi EL Nakheil, west EL Quseir, Eastern Desert,Egypt. Proceeding of the 3rd international conference for groundwater level control inside urbanized areas. Faculity of Engineering, Mansoura University. pp. 153–168

Khaled MA (2007) Geophysical and hydrogeological studies for the groundwater occurrences of Wadi Abu Zeran area, Eastern Desert, Egypt. 2nd international conference on the Geology of Thethys, Cairo University March 2007. pp. 463–474

Kuria D, Gachari M, Macharia M, Mungai E (2012) Mapping groundwater potential in Kitui District, Kenyausing geospatial technologies. Int J Water Res Environ Eng 4(1):15–22

Lewis SJ, Roberts J, Brodie RS, Gow L, Kilgour P, Ransley T, Coram JE, Sundaram B (2008) Assessment of groundwater resources in the broken hill region. Geosciences Australia Professional Opinion 2008/05

Mark DM (1984) Automatic detection of drainage networks from digital elevation models. Cartographica 21:168–178

Melton MN (1957) An analysis of the relations among elements of climate surface properties and geomorphology. Project NR 389-042 Tech. Rept. II, Columbia University, and Dept. of Geology, On Geog., R., Branch, New York

Miller VG (1953) A Quantitative geomorphic study of the drainage basin characteristics in the Clinch Mountain area, Virginia and Tennessee. Colombia University, Geology Dept., Project NR389-042, Technical Report No. 3

MPGAP: Mineral, Petroleum and Groundwater Assessment Project (1990) Progressive internal report, unpublished, (1984–1990), prepared by Desert Research Center (DRC)

Nag SK, Chakraborty S (2003) Influence of rock types and structures in the development of drainage network in hard rock area. J Indian Soc Remote Sens 31(1):25–35

NCEP (NOAA Climate Prediction Center, Reanalysis Version 2), (2015) Climate Reanalyzer, Climate Change Institute, University of Maine, USA, http://cci-reanalyzer.org Cited 1 March 2015

Pryde J, Osorio J, Wolfe M, Heatwole C, Benham B, Cárdenas A (2007) Comparison of watershed boundaries derived from SRTM and ASTER digital elevation datasets and from a digitized topographic map. ASABE (American society of agricultural and biological engineers), Paper No. 072093, Michigan, 1–10

Ramirez JA (2000) Prediction and modeling of flood hydrology and hydraulics, chapter 11, of Inland flood hazards: human, riparian and aquatic communities Eds. Ellen Wohl; Cambridge University Press

Rekha VB, Thomas AP (2007) Integrated remote sensing and GIS for groundwater potentially mapping in Koduvan Àr-Sub-Watershed of Meenachil river basin, Kottayam District, Kerala. School of Environmental Sciences, Mahatma Gandhi University, Kerala

Ruelleu S, Moreau F, Bour O, Gapais D, Martelet G (2010) Impact of gently dipping discontinuities on basement aquifer recharge: An example from Ploemeur Brittany, France. J Appl Geophys 70:161–168

Said R (1992) The geology of Egypt A A. Balkema—Rotterdam brookfield

Said R (1993) The river Nile: geology, hydrology and utilization, 2nd edn. Dar El Hilal, Cairo

Saraf AK (1999) A report on landscape modelling in gis for Bankura District, project sponsored by DST, NRDMS division Govt. of India

Schumm SA (1956) Evolution of drainage systems and slopes in badlands at Perth Amboy, New Jersey. Bull Geol Soc Am 67:597–646

Sewidan AS (2000) (MOPHOMET & HAZARD) Computer program of morphometric parameters and basins hazared degrees calculations, infiltration test calculation. Hydrology Department. Desert Research Center, Cairo, Egypt

Smith KG (1958) Erosional processes and landforms in Badlands National Monument, South Dakota. Geol Soc Am Bull 69:975–1008

Strahler AN (1953) Quantitative analysis of watershed geomorphology. Trans Am Geophys Union 38:913–920

Strahler AN (1964) Quantitative geomorphology of drainage basins and channel networks. In: Ven Chow Te (ed) Handbook of applied hydrology. McGraw Hill, New York, pp 4–76

Sturchio NC, Du X, Purtschert R, Lehmann BE, Sultan M, Patterson LJ, Lu ZT, Müller P, Igler T, Bailey K, Connor TPO, Young L, Lorenzo R, Becker R, El Alfy Z, El Kaliouby B, Dawood Y, Abdallah AMA (2004) One million year old groundwater in the Sahara revealed by Krypton81 and Chlorine36. Geophys Res Lett 31:L05503. doi:10.1029/2003GL019234

Subyani AM (2009) Hydrologic behavior and flood probability for selected arid basins in Makkah area, western Saudi Arabia. Arab J Geosci. doi:10.1007/s12517-009-0098-1

Sultan M, Sturchio NC, Gheith H, Hady YA, El Anbeawy M (2000) Chemical and isotopic constraints on the origin of Wadi El-Tarfa ground water, Eastern Desert, Egypt. Ground Water 38(5):743–751

Sultan M, Yan E, Sturchio N, Wagdy A, Abdel Gelil K, Manocha N, Becker R, Milewski A (2007) Natural discharge: a key to sustainable utilization of fossil groundwater. J Hydrol 335:25–36

Sultan M, Wagdy A, Manocha N, Sauck W, Abdel Gelil K, Youssef A, Becker R, Milewski A, El Alfy Z, Jones C (2008) An integrated approach for identifying aquifers in transcurrent fault systems: The Najd Shear system of the Arabian Nubian shield. J Hydrol 349:475–488

Sultan M, Yousef A, Metwally S, Becker R, Milewski A, Sauck W, Sturchio N, Mohamed A, Wagdy A, El Alfy Z, Becker D, Sagintayev Z, El Sayed M, Welton B (2011) Red sea rifting controls on aquifer distribution: constraints from geochemical, geophysical, and remote sensing data. Geol Soc Am Bull 123:911–924. doi:10.1130/B30146.1

UNEP (United Nations Environment Program, 2012) Annual report. ISBN: 978-92-807-3323-5 Available online at: http://www.unep.org/annualreport/2012/

USDA-SCS (1972) Hydrology. Section 4, Soil Conservation Service, National Engineering Handbook. U.S. Department of Agriculture-Soil Conservation Service: Washington, DC

USDA-SCS (1986) Urban hydrology for small watersheds. Soil conservation service, Natural resource conservation service technical release. 55, Available at: http://www.wcc.nrcs.usda.gov/hydro/hydro-tools-models-models-tr55.html

Voss CI, Soliman SM (2014) The transboundary non-renewable Nubian aquifer system of Chad, Egypt, Libya and Sudan: classical groundwater questions and parsimonious hydrogeologic analysis and modeling. Hydrogeol J 22:441–468

Wilson JL (1975) Carbonate facies in geologic history. Springer-Verlag, Berlin

Yousif M, Bubenzer O (2015) Geoinformatics application for assessing the potential of rainwater harvesting in arid regions,

El Daba'a area, Northwestern Coast of Egypt. Arab J. Geosci. doi:10.1007/s12517-015-1837-0

Youssef MI (1957) Upper Cretaceous rocks in Quseir area" Desert Institute, Egypt. Bull. VII 2:35–54

Youssef M, Pradhan B, Gaber AFD, Buchroithner MF (2009) Geomorphological hazard analysis along the Egyptian Red Sea coast between Safaga and Quseir. Nat Hazards Earth Syst Sci 9:751–766

Zaid SM (2009) Potential of flash flooding of the drainage basins of Quseir area and risk evaluation. Fourth Environmental Conference, Faculty of Science, Zagazig University, 1–16